AD-A147 643 AN ASSESSMENT OF THE POTENTIAL FOR TEMPERATURE AND MOISTURE RETRIEVALS FR.. (U) COLORADO STATE UNIV FORT COLLINS DEPT OF ATMOSPHERIC SCIENCE.. 1/1

UNCLASSIFIED D W HILLGER ET AL. SEP 82 AFGL-TR-82-0325 F/G 4/2 NL

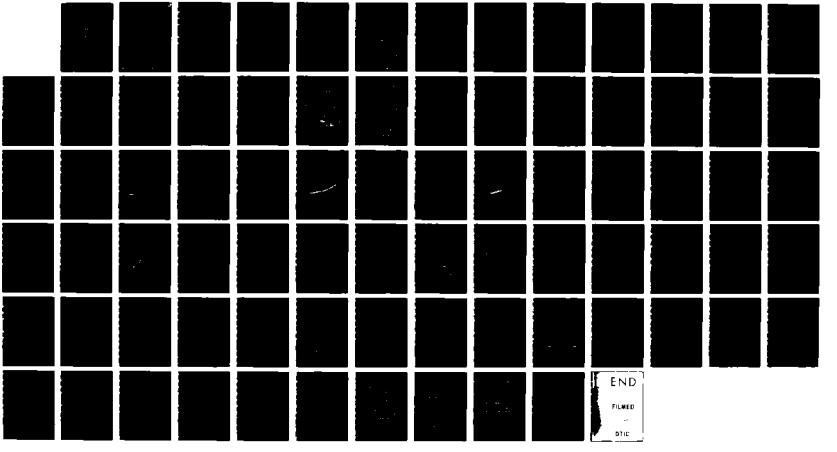

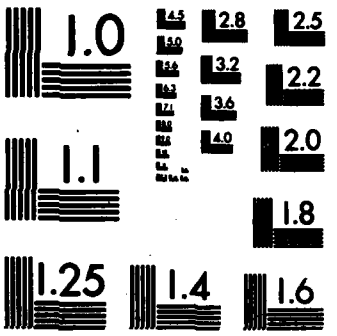

AFGL-TR-82-0325

AN ASSESSMENT OF THE POTENTIAL FOR TEMPERATURE AND MOISTURE RETRIEVALS FROM SSH-1 RADIANCES

Donald W. Hillger
Stanley Q. Kidder
Thomas H. Vonder Haar

Department of Atmospheric Science
Colorado State University
Fort Collins, CO 80523

September 1982

Scientific Report No. 1

AIR FORCE GEOPHYSICS LABORATORY
AIR FORCE SYSTEMS COMMAND
UNITED STATES AIR FORCE
HANSCOM AFB, MASSACHUSETTS 01731

This report has been reviewed by the ESD Public Affairs Office (PA) and is releasable to the National Technical Information Service (NTIS).

"This technical report has been reviewed and is approved for publication"

VINCENT J. FALCONE, JR.
Contract Manager

KENNETH R. HARDY
Chief, Satellite Meteorology Branch

FOR THE COMMANDER

ROBERT A. McCLATCHEY
Director, Atmospheric Sciences Division

Qualified requestors may obtain additional copies from the Defense Technical Information Center. All others should apply to the National Technical Information Service.

If your address has changed, or if you wish to be removed from the mailing list, or if the addressee is no longer employed by your organization, please notify AFGL/DAA/LYC Hanscom AFB, MA 01731. This will assist us in maintaining a current mailing list.

Do not return copies of this report unless contractual obligations or notices on a specific document requires that it be returned.

Unclassified

SECURITY CLASSIFICATION OF THIS PAGE *(When Data Entered)*

REPORT DOCUMENTATION PAGE	READ INSTRUCTIONS BEFORE COMPLETING FORM
1. REPORT NUMBER AFGL-TR-82-0325	2. GOVT ACCESSION NO. A147643
	3. RECIPIENT'S CATALOG NUMBER
4. TITLE *(and Subtitle)* An Assessment of the Potential for Temperature and Moisture Retrievals from SSH-1 Radiances	5. TYPE OF REPORT & PERIOD COVERED Scientific Report No. 1 1 June - 30 Sept. 1981
	6. PERFORMING ORG. REPORT NUMBER
7. AUTHOR(s) Donald W. Hillger Stanley Q. Kidder* Thomas H. Vonder Haar	8. CONTRACT OR GRANT NUMBER(s) F19628-80-C-0140
9. PERFORMING ORGANIZATION NAME AND ADDRESS Colorado State University Department of Atmospheric Science Fort Collins, Colorado 80523	10. PROGRAM ELEMENT, PROJECT, TASK AREA & WORK UNIT NUMBERS 62101F 767013AB
11. CONTROLLING OFFICE NAME AND ADDRESS Air Force Geophysics Laboratory Hanscom AFB, MA 01731 Monitor - Vincent Falcone - LYS	12. REPORT DATE September 1982
	13. NUMBER OF PAGES 75 pages
14. MONITORING AGENCY NAME & ADDRESS*(if different from Controlling Office)*	15. SECURITY CLASS. *(of this report)* Unclassified
	15a. DECLASSIFICATION/DOWNGRADING SCHEDULE

16. DISTRIBUTION STATEMENT *(of this Report)*

Approved for public release; distribution unlimited

17. DISTRIBUTION STATEMENT *(of the abstract entered in Block 20, if different from Report)*

18. SUPPLEMENTARY NOTES

*University of Illinois

Department of Atmospheric Science

19. KEY WORDS *(Continue on reverse side if necessary and identify by block number)*

Satellite Soundings
Special Sensor H (SSH)
Temperature and Moisture Retrievals
Statistical Regression

20. ABSTRACT *(Continue on reverse side if necessary and identify by block number)*

Several aspects of the Special Sensor H (SSH-1) infrared sounding problem are addressed. These aspects relate to the objective of assessing the current temperature and moisture retrieval capabilities from real SSH-1 radiances. The outcome of this will be the improvement of the retrievals, especially with respect to moisture information. A second goal is the improvement of the cloud detection and cloud elimination problems. → cont

(continued on reverse side)

DD FORM 1 JAN 73 1473

Unclassified

SECURITY CLASSIFICATION OF THIS PAGE *(When Data Entered)*

cont

Radiance noise levels are statistically estimated and are found in some cases to be larger than those expected based on pre-flight testing but are of the same order of magnitude as the predicted sensitivities. These results signal that the SSH-1 instruments were performing roughly as expected. The lack of moisture retrieval capability is then either due to the improper selection of channels or their improper use in the retrieval process. Of interest is that eigenvector analysis shows that within the 15 CO_2 and H_2O channels there are only seven significantly independent pieces of information.

The scan angle correction problem is also addressed, as well as cloud elimination techniques. Corrections for both of these problems are needed in the application of a statistically-based retrieval scheme. A single field-of-view technique using the two window channels which will be available on SSH-2 shows the most promise at cloud detection.

The results of applying a simple regression retrieval scheme to obtain temperatures and moisture are found to be comparable to results noted by others. However, the performance is below that required by Air Force Global Weather Central (AFGWC). Attempts at implementation of an iterative retrieval system lead to the adaption of various sources of transmittance software to the SSH-1 channels. The iterative retrieval, however, was abandoned because of the need for a scheme which requires less computer time. Computing expense and time limitations must also lead to judicial selection of SSH channels for input to a simple regression technique. This new software will also be adapted to improvements in channel selection in future SSH-2 data, especially with respect to the increased number of highly transparent and window channels.

TABLE OF CONTENTS

LIST OF FIGURES

LIST OF TABLES

ACKNOWLEDGEMENTS

The results covered in this report were made possible by the assistance of the following AFGL personnel: Mr. Vincent Falcone, Dr. Kenneth Hardy, Dr. Robert McClatchey and Dr. J. I. F. King. Several discussions with AFGWC personnel were also very helpful, especially Maj. Stephen Pryor (formerly of AFGWC) who provided both software and SSH-1 data. Dr. Michael Weinreb also provided software used operationally at NOAA/NESDIS in Washington, D.C. Mr. Alan Lipton reviewed the manuscript.

Drafting was provided by Judy Sorbie and word processing by Robin Wilson and Loretta Stevens.

This research was sponsored by the Air Force Geophysics Laboratory (AFGL), Hanscom Air Force Base, under Contract No. F19628-80-C-0140.

1.0 INTRODUCTION

This report addresses several aspects of the remote sounding problem with respect to the use of SSH-1 (Special Sensor H) infrared satellite data. The SSH-1 instrument was carried on four Defense Meteorological Satellite Program (DMSP) satellites and was operational from 1976 to 1980. During that time SSH-1 data was intended to be used operationally in support of weather analysis and forecasting at Air Force Global Weather Central (AFGWC). However, several problems with both the data and retrieval systems have caused serious deficiencies in the use of the SSH-1 soundings.

With the future launch of SSH-2 (modified SSH-1) instruments, some filter changes will be instituted. However, the instrument will still be similar to the SSH-1 design. The lack of success in the use of SSH-1 data must, therefore, be addressed.

The contract under which this work was completed covers five (5) main areas where help is needed and can be provided. The first two of these objectives are addressed in this report. They are briefly:

1. The assessment of current statistical retrieval schemes as used by AFGWC and applied to synoptic scale data. Assistance with implementation of new techniques and suggestions as to development or modification of new techniques to be applied as needed.

2. The assessment of the cloud-contamination problem, especially in statistical retrieval methods. This includes comparisons with current cloud elimination techniques as applied to infrared data. Such techniques are of vital importance unless enough sounding resolution is available to obtain some clear column radiances.

Several topics related to these two objectives will be discussed in the following sections.

Section 2 deals with the SSH-1 radiances. Serious consideration was given to the satellite measurements, so as not to overlook any basic deficiencies which might exist. The SSH radiances were subjected to statistical tests which uncovered some previously known problems, such as the obstruction in the field-of-view. A statistical structure function analysis also allowed an estimation of the radiance noise levels. The noise levels for many channels compared favorably w the predicted noise levels. This signifies that the SSH-1 measureme of the expected quality, and any deficiency in retrieval accuracy is not due to the radiances themselves, although the selection of the channel filter responses may not be optimal.

Section 3 covers an important aspect of any satellite data which are obtained from scanning radiometers. The changing viewing angles cause an extra variation in the measurements due to changing atmospheric path lengths, especially for those channels which are least transparent to the atmosphere. One problem with the previously used zenith angle corrections was uncovered and a solution is proposed.

In Section 4 the cloud problem is addressed. Two methods are presented to deal with clouds by simple means. One method uses simple radiance thresholds to detect cloudy values. The other method uses the different spectral qualities of the two window channels which will be available on SSH-2 to determine both cloud amount and temperature (or height). These techniques are needed mainly to eliminate cloudy values from consideration in the retrieval process because infrared measurements are severely limited in cloudy situations.

Section 5 assesses a regression retrieval scheme as applied to SSH-1 for both temperatures and moisture. Testing was done on both dependent data sets (those used to develop the regression coefficients) and independent data sets (other than those used to develop the regression coefficients). On independent data the retrieval 'errors' are greater than on dependent data, as expected. However, the results show that sufficient information content does exist in the SSH-1 radiances to determine temperatures at most levels, with large positive explained variances. In other words, the 'error' variance is much less than the total variance. The moisture results also show positive explained variances at the lowest atmospheric levels, indicating that moisture information does reside in the SSH-1 radiances (although the moisture information content is less complete than the temperature information). This is contrary to unpublished findings of poor or non-existent moisture retrieval capabilities at AFGWC. Their poor results may be linked to the statistical data base used for regression coefficient development or to errors in the RAOBs or radiances.

Finally, Section 6 deals with transmittance software which was developed for SSH-1. The main reason for this software development was to be able to apply iterative or minimum-information retrieval schemes to SSH-1 radiances. (Such retrieval techniques do not require paired satellite-RAOB data as a statistical base.) The software combines techniques from various sources for the H_2O, CO_2, and window channels and it remains to be thoroughly tested. Development was discontinued in

lieu of simpler methods for retrieval, since both the iterative retrievals and transmittance calculations require extensive computer resources.

2.0 STATISTICAL RADIANCE ASSESSMENT

The assessment of SSH-1 radiance quality is an approach to the problem of determining maximum temperature and moisture retrieval capabilities. The real (not simulated) SSH-1 radiances tested were calibrated at AFGWC but uncorrected for zenith angle variations. Cloud contamination was eliminated through procedures which will be discussed in the following section. Statistical structure function analysis is then used to obtain an estimate of the noise level for each radiance channel. These noise levels are then compared to those predicted using design specifications and measurements made before launch of the spacecraft (Yoder, 1975; Klein et al., 1976).

Previous work using structure function analysis of noise levels (Hillger and Vonder Haar, 1979) was done for Vertical Temperature Profile Radiometer (VTPR) radiances from the NOAA-4 satellite. Those results gave estimated rms radiance noise levels ranging from the predicted radiometer sensitivities to values several times higher for channels which sense lower in the troposphere. Estimated noise levels presented here for the SSH-1 radiances show similar results. With the atmospheric variability eliminated these estimated noise levels should be directly translatable into temperature retrieval capability assuming that no bias exists between retrieved and actual temperatures, but that step has not yet been made.

2.1 Noise-Level Theory

The idea of obtaining noise levels of satellite measurements from

structure function analysis is considered equivalent to determining noise levels from repeated measurements of the same field-of-view (FOV). Since the satellite does not normally measure the same FOV more than once per sounding channel it is difficult to obtain noise-level data from such a set of measurements. The satellite instrument is continually scanning the surface of the earth in adjacent FOVs. For the SSH radiances these spots are approximately 60 km in diameter, or equivalently 60 km between spot centers at nadir along the scan track. The spacing, however, does increase with increasing scan angle. Also, since the earth's atmosphere and surface each change in both temperature and emittance characteristics from FOV to FOV these additional variations are introduced on top of the expected variations due to noise (including instrumental noise, data-digitizing noise, and data transmission noise).

These atmospheric and surface variations can be reduced in a statistical sense by analyzing an extremely large number of measurements. The mean change from one FOV to the next will then be evident. This mean difference will be a combination of both the real horizontal variation between the two spots and the noise in the two measurements. Therefore, by extrapolating this mean measurement difference as the FOV separation distance goes to zero, all horizontal variations are eliminated and the only variations that remain are due to noise. With all atmospheric and surface variation due to horizontal gradient eliminated, this process is equated to obtaining repeated measurements of the same FOV.

Gandin (1963) was among the first to use structure function analysis as an indirect means of estimating errors in meteorological

data sets. The spatial structure function is a measure of the mean-squared difference in measurements as a function of their separation distance. The analysis can be accomplished on a single synoptic situation in theory, but that is true only if a sufficiently large number of data points are available, such as high-density satellite measurements. In this study not only was the statistical sample large, but satellite radiances from several passes over two different regions of the earth were analyzed to further eliminate any bias due to a one-look analysis.

Purely random errors lead to an exaggerated value for the structure function by an amount equal to a double mean-squared error ($2\sigma_e^2$) in the measurements. Each of the measurements in a pair contributes half of this uncertainty. Of course, homogeneity and isotropy with respect to the structure function are assumed. In other words, the fields may not be homogeneous or isotropic, but the noise on the measurements is assumed to be. This is most likely to be true in a large sample or variation of synoptic situations. The sample used here is considered to be sufficiently large that the results are only slightly dependent on the sample under study. Previous results (Hillger and Vonder Haar, 1979) showed how the structure function varied with the synoptic situation, but the error analysis here does not show the variation evident in the individual synoptic situations since most of the variation due to the atmosphere and surface is extrapolated out of the individual structure functions.

2.2 An Example of Structure Analysis

The satellite radiances that were analyzed were obtained at several local times on 5 and 6 November 1979. The SSH-1 radiances were obtained

from three DMSP satellites (WX3536, WX4537, and WX5539) which take measurements at approximately local 9, 7, and 11, respectively. The areas considered were a 15° latitude by 15° longitude area from 30° to 45°N and 90° to 105°W centered over western Oklahoma (Figure 2.1) and a 20° latitude by 20° longitude area from 10° to 30°N and 145° to 165°W centered over Hawaii. Each satellite pass contained a sample of up to approximately 200 radiance measurements for each channel considered. Statistical pairing then provided about 400 pairs of adjacent FOVs and larger numbers of pairs of FOVs separated by greater distances. Briefly, the paired values were categorized into range gates of 60 km width, with divisions at 30, 90, 150, 210 km etc. Paired FOVs would therefore fall into all but the first range gate (less than 30 km). This range gate spacing allowed the paired FOVs to be categorized into natural divisions. However, adjacent diagonal pairs and spots separated by several FOVs would fall into the appropriate range gates, and the divisions would become less clear for larger separations. Details of the structure equations are provided in previous work (Hilliger and Vonder Haar, 1979). Running sums kept track of the paired values in each range gate and the separation distance, so the results represent a 1-dimensional structure (mean-squared difference) along with a mean separation distance for the pairs in each range gate.

One example of a structure function for SSH-1 channel E1 at 668 cm^{-1} (CO_2 Q branch) is shown in Figure 2.2. This graph shows results of the structure analysis on the Hawaii sector outlined above. A total of 5 satellite passes went into the calculations with over 700 radiances in the analysis. Structure values are given at mean separation distances of approximately 60, 120, 180, 240 km etc. These are halfway between

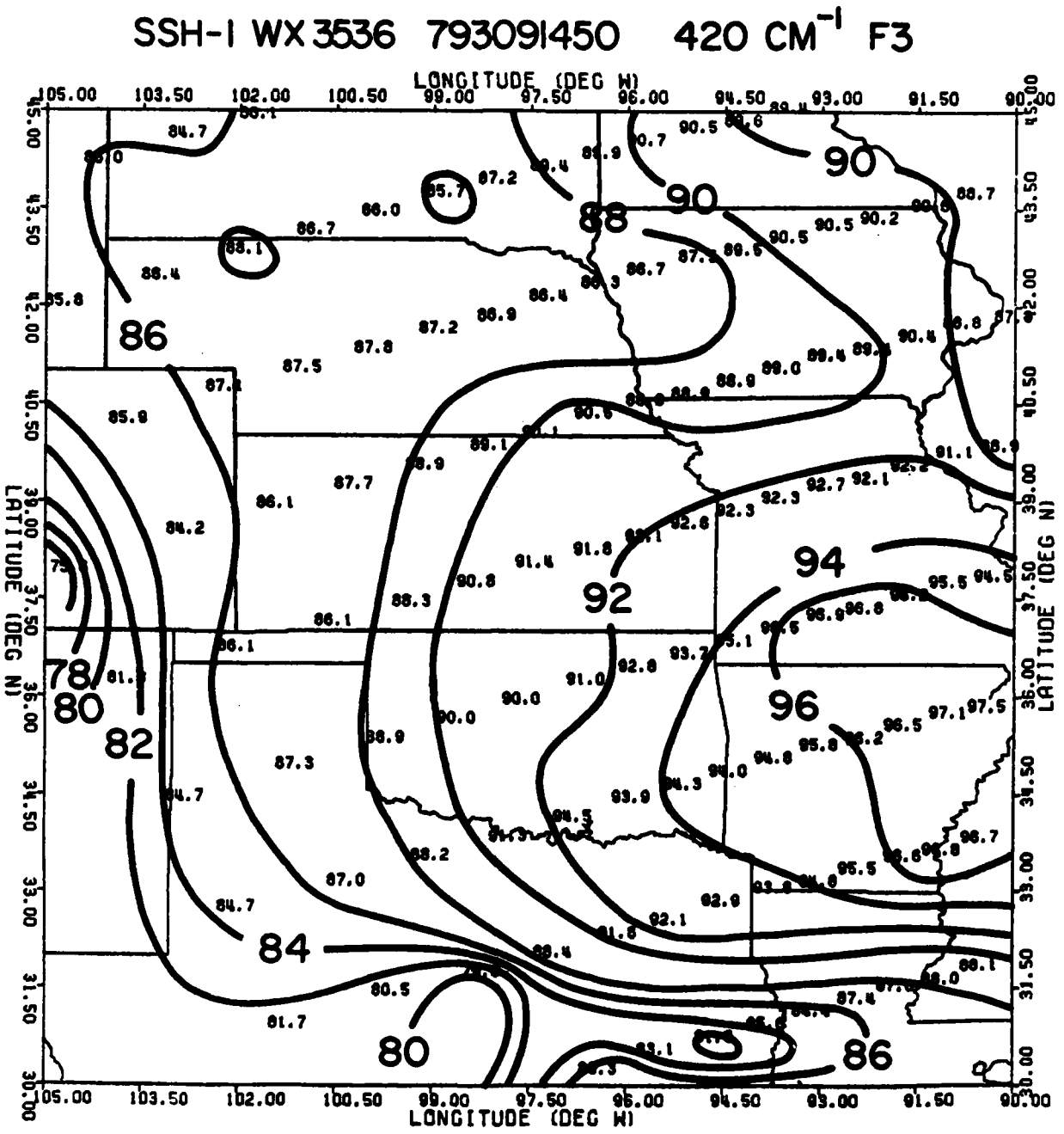

Figure 2.1 An example of the SSH-1 scan pattern and resolution. The radiances are for channel F3 (420 cm^{-1}) over the mid-latitude sector chosen for study.

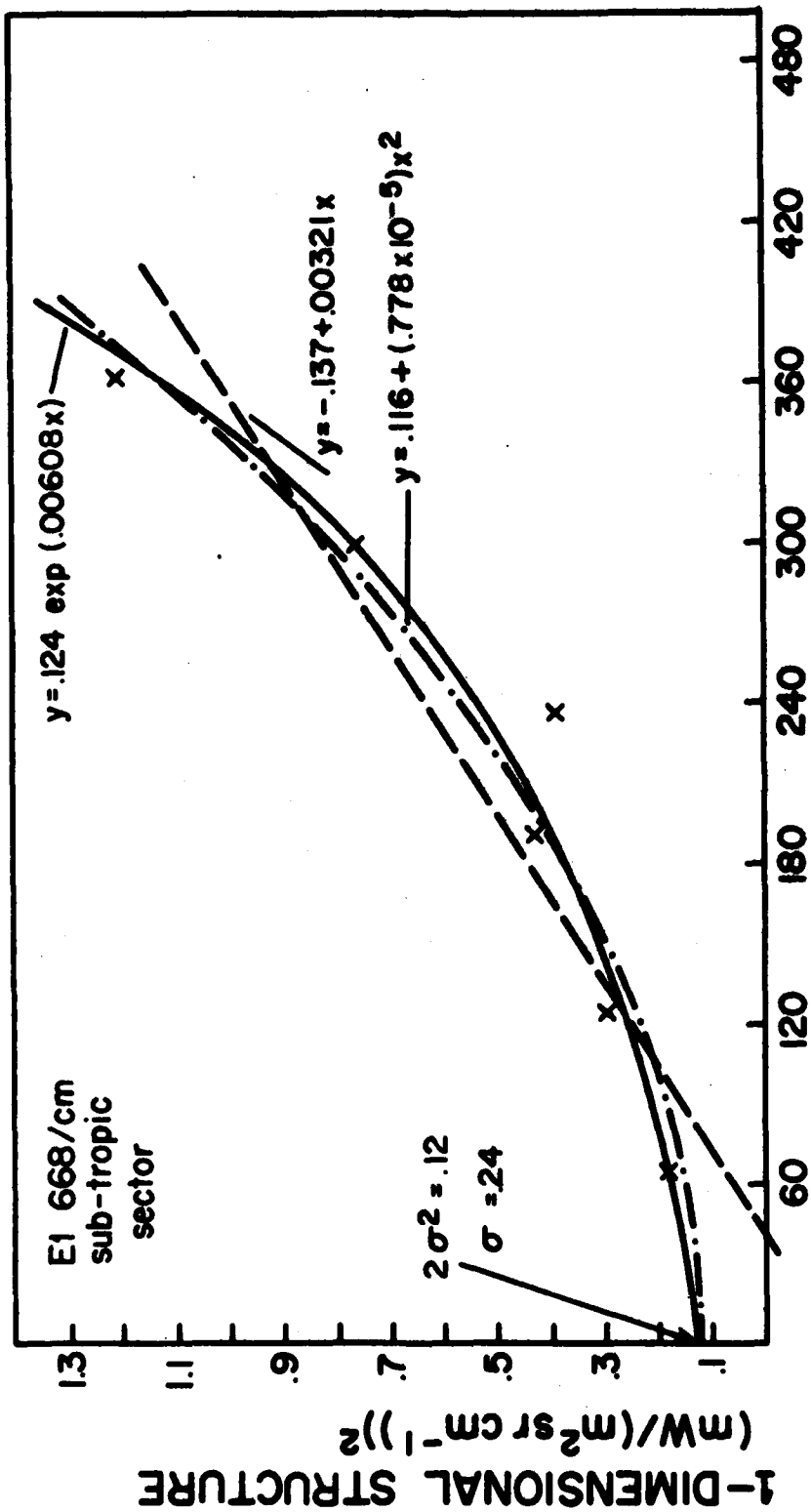

Figure 2.2 An example of SSR-1 radiance structure for channel E1 (668 cm^{-1}) for the sub-tropic (Hawaii) sector. Three curves have been fitted to the structure values by least-squares regression in order to determine the most probable intercept at zero separation distance.

the range gate limits. No paired FOVs were separated by less than 30 km so the first occupied range gate from 30 to 90 km contained all adjacent pairs along the scan line. Adjacent FOVs between one scan line and the next are first included in the range gate from 210 to 270 km because of the 220 km mean separation between scan lines. This uneven spacing between along-scan and cross-scan pairs presented some analysis problems, but these were overcome by appropriate selection of the range gates. (See Figure 2.1 for the SSH-1 scan pattern.) The X's in Figure 2.2 are the actual (mean-squared difference) values. The structure is therefore normally an increasing function of distance, but the decrease at 240 km is probably due to the effect of cross-scan pairs added at this distance. Structure plots of some other channels did not show this feature. The decrease also may be due to the fact that the radiances were not corrected for zenith angle variations. Along-scan values would contan such variations and cross-scan values would not. However, it is felt that this effect is small in cases where the natural atmospheric and surface variations are large, since those variations will in general be random with respect to separation direction.

Each structure value represents the mean-squared difference between values at that separation. Increasing structure with distance, therefore, represents the mean gradient in the field of analyzed radiances. This gradient is then eliminated by extrapolation of the strucuture to zero separation distance (finding the intercept with the structure axis). This intercept was found by the least-squares fitting of several lines to the actual structure values. The lines fit to the values in Figure 2.2 were a linear, a symmetric quadratic, and an

exponential with the forms:

$$Y = A + Bx \tag{2.1}$$

$$Y = A + Ox + Cx^2 \quad (B = 0) \tag{2.2}$$

$$Y = A \exp(Bx) \tag{2.3}$$

The A, B, and C coefficients found by least-squares for each line are shown on the graph. The lines were fitted to the structure values only up to a mean separation of 360 km. This cutoff was used since the structure beyond this point decreased and would require the fit of a more complex curve. Other curves were also fit to these points as will be mentioned, and the cutoff for curve fitting with distance was a function of the radiance channel and synoptic situation.

The linear least-squares line in Figure 2.2 proved to have a negative structure intercept at zero separation distance, so that line was not considered a good fit since the mean-squared difference (structure) values are all required to be greater than zero. However, the symmetric quadratic and exponential curves both had a similar intercept of 0.12 $(mW/(m^2 sr\ cm^{-1}))^2$ at 0 km. This translates to a mean rms noise of 0.24 $mW/(m^2 sr\ cm^{-1})$ since the former value is the double mean-squared noise, one component coming from each of the paried values. This value is considered the most probable intercept since it is confirmed by two least-squares lines. A potential advantage to the symmetric quadratic is the fact that its slope is defined as zero at

zero separation distance. The structure should theoretically decrease to such a plateau as the minimum noise level is reached. However, for some situations the plateau may be reached quite abruptly.

2.3 Results of Structure Analysis

Table 2.1 shows the results for each of the two regions studied as compared to the predicted noise levels for all of the SSH-1 radiance channels. The goal here was to see how the obtained radiance noise levels compared to those predicted. The two regions under study were kept separate to see if each had different characterisitcs or if one region confirmed the values obtained by the other region. The pressure at the weighting function maximum for each radiance channel is also shown. Channels which peak lower in the atmosphere are expected to have larger structure functions due to more atmospheric and surface variability. This atmospheric variability should be mostly removed by the extrapolation process to zero separation distance. However, in the case of lower tropospheric channels, especially the window channel, this atmospheric and surface variability may not be completely eliminated. Small cloud amounts and low clouds are especially hard to detect. This will be addressed further in a following section.

The noise levels obtained by structure analysis compared favorably with the predicted noise levels given by Yoder (1975) and by Klein, et al (1976). The numbers given by these sources are presumably for only one satellite and the results here are composited for three satellites. This was not meant to be an exhaustive noise analysis, only to see if the noise levels obtained here were grossly different than the predicted values, which did not seem to be the case.

Table 2.1

Summary of SSH-1 Radiance Noise Levels

Channel	Center Wavenumber (cm^{-1})	Band	Approximate Peak Pressure+ (mb)	NESR* ($mW/m^2 sr\ cm^{-1}$)	Most Probable Extrapolated Structure Noise Mid-latitude ($mW/m^2 sr\ cm^{-1}$)	Most Probable Extrapolated Structure Noise Sub-tropics ($mW/m^2 sr\ cm^{-1}$)
F8	353	H_2O	400	.33	.35	.50
F1	355	H_2O	500	.25	.21	.44
F7	374	H_2O	500	.18	.23	.51
F2	397	H_2O	500	.16	.24	.49
F6	408	H_2O	850	.14	.20	.55
F3	420	H_2O	600	.12	.27	.52
F4	442	H_2O	700	.09	.31	.59
F5	535	H_2O	surface	.15	.12	.56
E1	668	CO_2	30	.30	.22	.24
E2	677	CO_2	70	.09	.06	.11
E3	695	CO_2	150	.10	.06	.07
E4	708	CO_2	350	.11	.12	.26
E5	725	CO_2	500	.11	.22	.11
E6	747	CO_2	1000	.12	.13	.13
W2	835	window	surface	.11	.39	.59
Z1	1022	O_3		.05	.19	.20

+ for 1962 U.S. Standard Atmosphere

* Noise Equivalent Spectral Radiance (Yoder, 1975; Klein et al, 1976)

The H_2O channel noise levels for the mid-latitude region compared favorably with the predicted values. Even the larger predicted noise for the F8 channel (353 cm^{-1}) did show up in the structure analysis. The H_2O radiance noise levels for the sub-tropic region were all about 0.5 $mW/(m^2 sr\ cm^{-1})$. This behavior is unexplained but thought to be a function of the more moist synoptic situation compared to the mid-latitudes. These values, however, were still of the same order of magnitude as those predicted.

For many of the CO_2 channels the noise levels for the mid-latitude and sub-tropic regions showed reasonable comparison to predicted values, however, some noise levels were about 2 times the predicted noise (reference channels E4 and E5). Many of these noise values were obtained by more complex extrapolations than the ones for the example shown in Figure 2.2. The most common fit was for the form:

$$Y = A \exp(Bx + Cx^2) \tag{2.4}$$

This is not a symmetric function but it did many times provide a lower noise level than the other functions used in the example. A choice between the intercepts for all the fitted curves was made for the most probable intercept among the available choices. The lowest intercept was chosen if any one value was not confirmed by two or more fitted lines.

The window and ozone channels also showed higher noise than predicted, but the differences are not unreasonable since the window channel especially may contain some unexplained surface variability in adjacent FOVs. Only gross discrepancies would be of concern. But, enlarged noise levels, if true, may signify some need for consideration.

For example, a minimum information retrieval technique depends on statistical knowledge of radiance noise levels. An error in this value does effect the retrieval solutions.

2.4 Eigenvector/value Analysis

Since many of the H_2O channels are rather opaque there is much redundency in the radiances used in any retrieval program. Therefore, an analysis of the same limited data sets as used in the structure analysis was performed, which showed that only 3 eigenvalues explain over 99.5% of the variance in the H_2O channels. The other 5 eigenvalues add only an insignificant amount of information. This indicates that no more than 3 independent pieces of information exist among the 8 H_2O channels.

For the CO_2, window, and ozone channels the number of significant eigenvalues needed to explain over 99.5% of the total variance is again only 3. This means that no more than 3 independent pieces of information exist in the 6 CO_2, window, and ozone channels. Much of this interdependence among channels is caused by the tendency for atmospheric variables to be correlated in the vertical, as well as the broad weighting functions for each channel.

3.0 SCAN-ANGLE CORRECTION PROBLEM

In working with the SSH-1 radiances, the problem of variations due to changing satellite viewing angles was anticipated. Some radiance channels would experience limb darkening (those which obtain their main contribution from the troposphere) and others would experience limb brightening (those which obtain their main contribution from the stratosphere). This introduces an extra variation in addition to changes due to different atmospheric conditions between adjacent satellite measurements. By eliminating this variation we can treat all measurements as if they originated at a common (zero) zenith angle.

The software documentation provided by AFGWC gave a 3rd-order polynomial correction for scan-angle variations of the form:

$$\text{Ratio} = A_0 + A_1\ \text{Zen} + A_2\ \text{Zen}^2 + A_3\ \text{Zen}^3 \qquad (3.1)$$

where Ratio is the factor by which to multiply the radiances at the specified zenith angle to correct them to nadir. Such a correction is necessary when working with radiances from radiometers on nearly all satellites. The radiances should all be converted to a common (zero) zenith angle, or alternately, the zenith angle variations should be taken into account by other means, such as in the retrieval process.

Typically the scan angle variations follow a cosine or secant function since the atmospheric transmittances are a function of the secant of the viewing (or zenith) angle with respect to the earth's

normal vector. The transmittance calculations follow a formula:

$$\tau = \tau_o \exp[\sec(Zen)] \qquad (3.2)$$

where τ_o is the transmittance at zero zenith angle and τ is the transmittance at zenith angle Zen. This simple relationship, however, applies only to a single atmospheric level and a more complex relationship evolves as the radiative transfer equation is integrated through the different density layers of the atmosphere.

Past work of the authors using VTPR data revealed that the zenith angle correction was linearly related to the square root of the secant of the zenith angle (see also Duncan, 1977). The secant of the zenith angle is a logical choice for the independent variable because of the above explanation relating transmittance variations to zenith angle.

For the SSH-1 radiance channels the zenith angle corrections as determined by polynomial coefficients provided by AFGWC are plotted in Figure 3.1. The required radiance changes are the polynomial ratios multiplied by the mean radiance in each channel. All channels except F8 (353 cm^{-1}) gave a near-zero correction at zero zenith angle. (There should be no change at nadir; such a change would bias the measurements.) However, channel F8 added about 4 $mW/(m^2 sr\ cm^{-1})$ at zero zenith angle. This introduced a bias of about +5% to the mean value of about 73 $mW/(m^2 sr\ cm^{-1})$ for this channel.

Even with this bias removed, by making the zero order polynomial coefficient equal to 1., the F8 polynomial had a shape not typical of the other H_2O channels, as shown in Figure 3.2. These figures were brought to the attention of AFGWC personnel. Their response was that the polynomials were created by fitting curves to large samples of

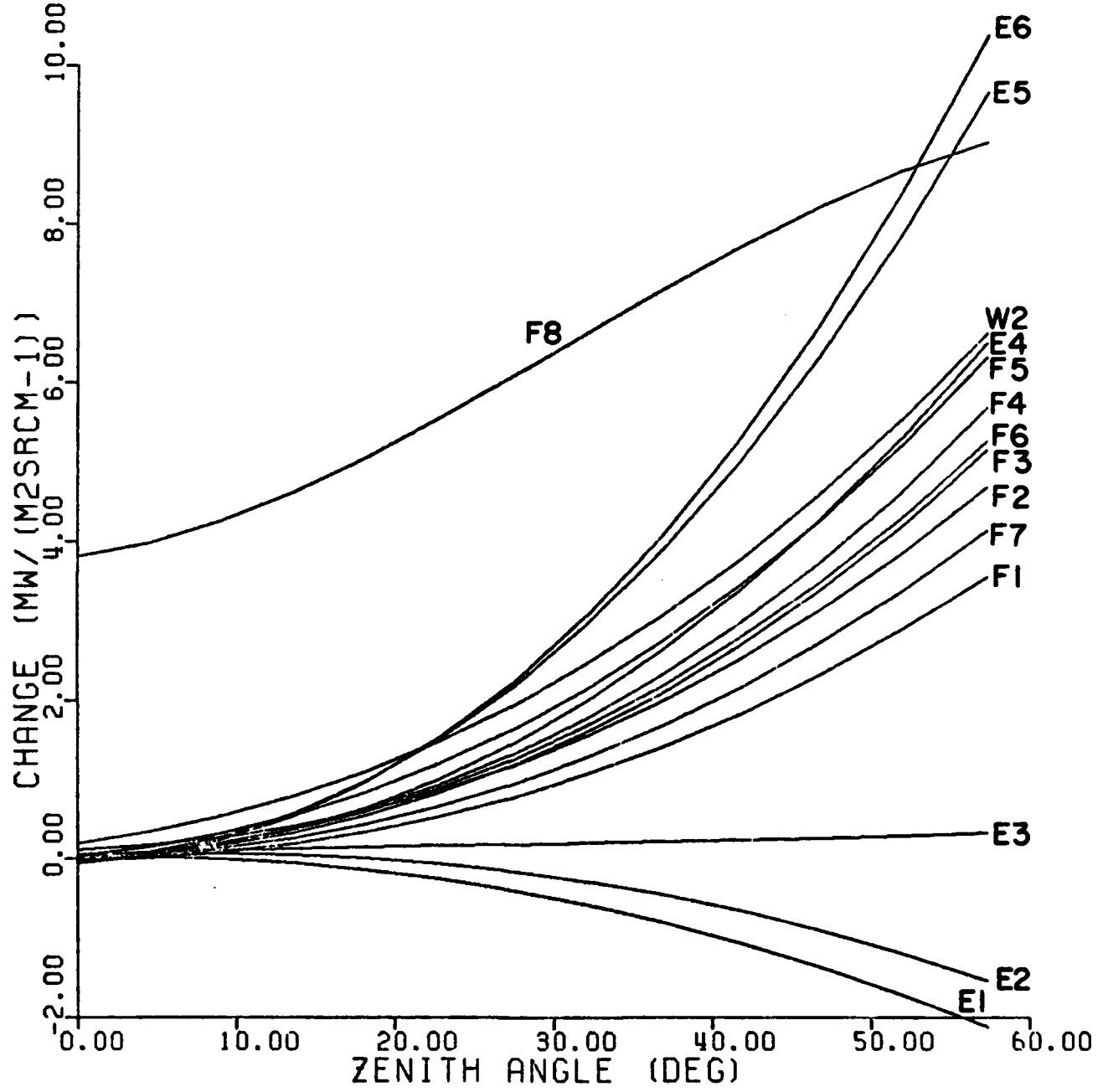

Figure 3.1. Zenith angle corrections applied to mean SSH-1 radiances as in AFGWC subroutine ZENCOR.

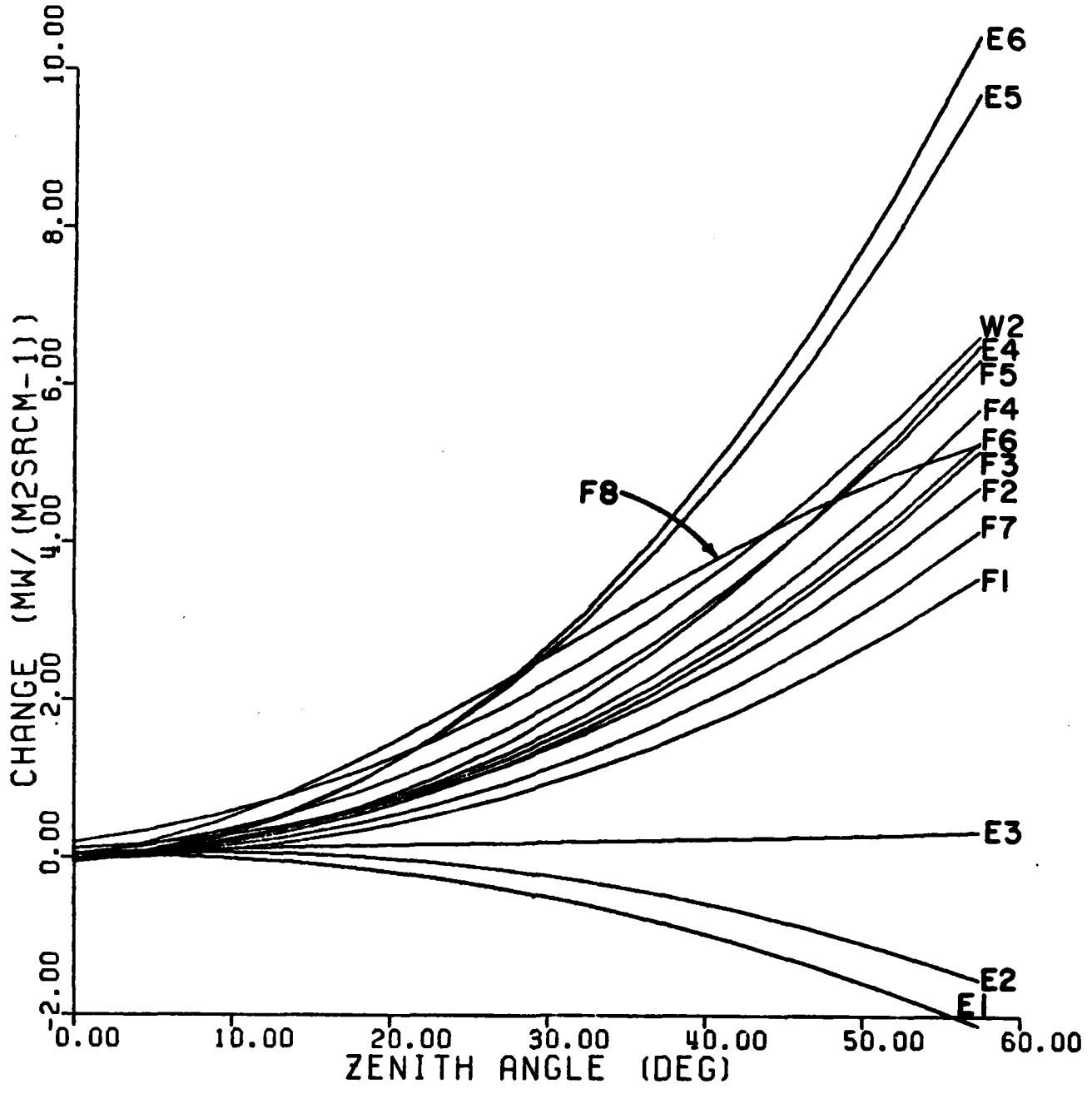

Figure 3.2. Zenith angle corrections applied to mean SSE-1 radiances with F8 zero-order coefficient = 1.

satellite measurements averaged at each scan position. The polynomials were based on data from satellite F3 (not to be confused with channel F3). The average F8 channel response with zenith angle was especially erratic and the polynomial which was fitted to the zenith angle changes reflected this erratic behavior. No other explanation for the F8 bias was given.

In an attempt to recreate the polynomials, the SSH-1 radiances from at least two time periods were analzyed to determine the corrections necessary to take the zenith angle variations out of the several channels. These two time periods were 6-7 November 1979 and 14-15 January 1979. The analysis required considerable computer time since each period consisted of many orbits of data. Some problems arose in reading the November 1979 data, but the January 1979 data provided a good statistical sample. Over 55 thousand scan spots were anlyzed of which over 27 thousand were considered non-cloudy.

Table 3.1 gives the mean and standard deviation for each of the radiance channels as compiled from the 14-15 January 1979 SSH-1 data supplied to us by AFGWC. Effort was made to eliminate bad radiances [especially those caused by the glare obstructor (glob) problem (Valovcin, 1980)]. Also, cloudy radiances were eliminated by using a minimum threshold of 85 $mW/(m^2\ sr\ cm^{-1})$ for the 12 μm window channel (835 cm^{-1}). Radiance values lower than this threshold were considered to be cloud contaminated.

After the cloudy values were eliminated by the threshold method, polynomials similar to Equation 3.1 were fit to this data and are plotted in Figure 3.3. The required radiance changes are similar to those provided by AFGWC. However, most of the F channels show similar

Table 3.1

SSH-1 radiance statistics for 14-15 Jan 1979 and corrections at 57° zenith angle for polynomials fit to the Jan 79 data set and for polynomials provided by AFGWC

		Jan 79		Polynomial Correction at 57°	
Channel	Wavenumber	Mean	Std. Dev.	Jan 79	AFGWC
	(cm^{-1})		($mW/(m^2\ sr\ cm^{-1})$)		
F8	353	73.	4.0	3.4	5.2
F1	355	77.	3.9	3.3	3.6
F7	374	84.	4.4	3.6	4.1
F2	397	88.	4.6	3.7	4.7
F6	408	99.	5.3	3.7	5.3
F3	420	95.	5.2	3.7	5.1
F4	441	101.	5.7	4.1	5.7
F5	535	116.	6.6	4.2	6.3
E1	668	57.	3.0	-2.3	-2.1
E2	677	44.	2.6	-2.2	-1.5
E3	695	42.	2.6	1.4	0.3
E4	708	58.	2.9	7.7	6.5
E5	725	78.	4.6	9.6	9.7
E6	747	91.	5.9	8.7	10.4
W1	835 (two looks)	108.	10.7	3.5	—
W2	835 (one look)	108.	10.7	3.4	6.6
Z1	1022	59.	7.6	7.9	—

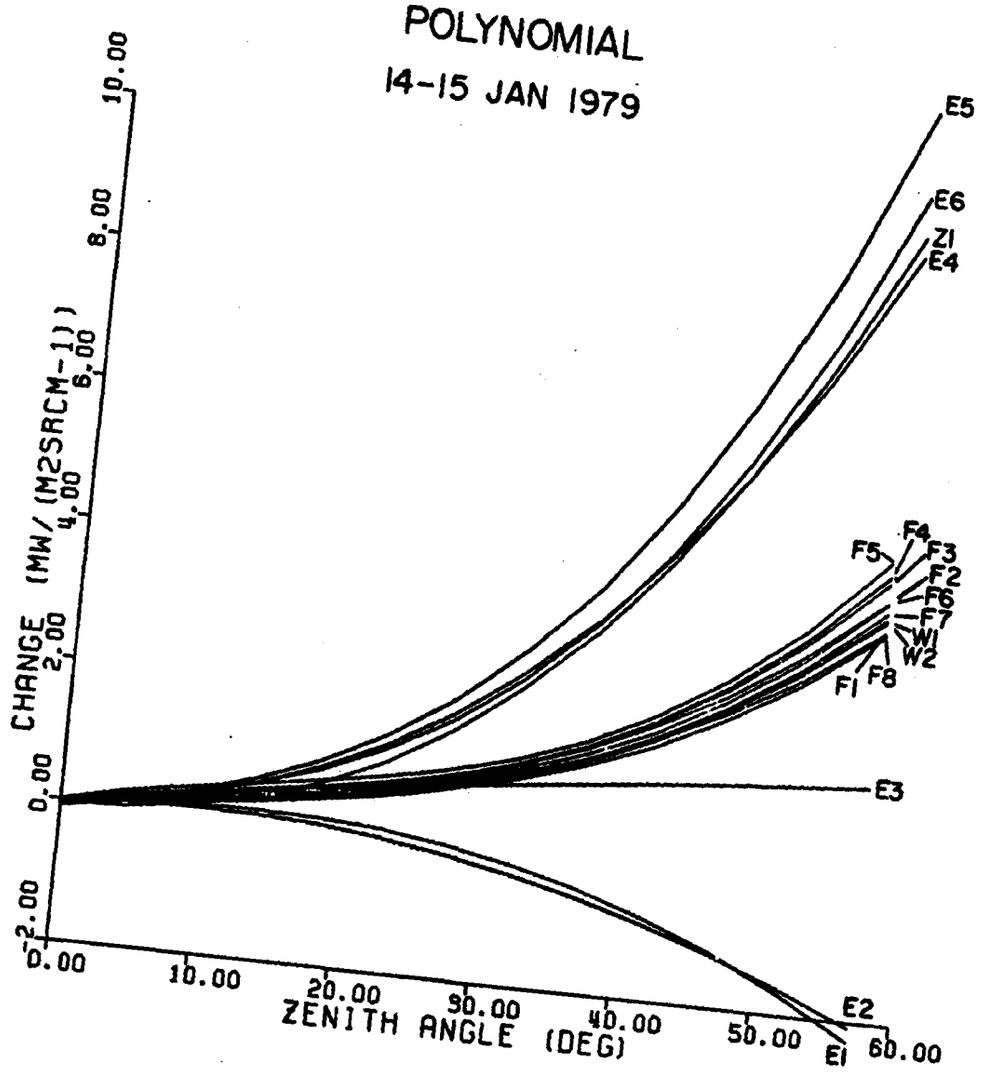

Figure 3.3. Required SSH-1 radiance change as a function of zenith angle for polynomials fit to mean SSH-1 radiances for all orbits on 14-15 January 1979.

changes and are clustered together with the window channels W1 and W2 (two and one looks respectively). The F channel zenith angle changes in Figures 3.1 and 3.2 are more spread out, but this difference in spread is most likely due to the different data samples which went into each analysis.

The last two columns of Table 3.1 give the polynomial corrections specified for the maximum zenith angle of 57°. The 'Jan 79' column gives the correction for polynomials fit to the SSH-1 data for which the statistics were given in the third and forth columns of Table 3.1. The 'AFGWC' column gives the same correction (at 57°) for the polynomials provided by AFGWC (on an unknown data set). The 'Jan 79' data includes passes from two satellites (WX3536 and WX4537), whereas the 'AFGWC' polynomials were fit to only one satellite (F3). Regardless of these differences, the corrections specified by the polynomials for the two data sets are within about 2 mW/(m^2sr cm^{-1}) for most of the F (H_2O) and E (CO_2) channels. The largest discrepancies occurred for the most transparent channels (F5, E6, and W2) and for channel F8 where the AFGWC polynomial is assumed to be in error.

A solution to this problem is to assume that the polynomial correction for F8 is similar to that for F1, the nearest H_2O channel in terms of wavenumber and sensing depth in the atmosphere. The required radiances changes for the Jan 1979 data are similar for channels F8 and F1, but rather than using the polynomials fit to this data set it was assumed to be safe to apply the AFGWC polynomial for F1 to channel F8. This produces a radiance correction of 3.4 (instead of the previous value of 5.2) mW/(m^2sr cm^{-1}) at the maximum zenith angle of 57°.

It was also decided that the polynomials used to correct the SSH-1

radiances should produce no bias at zero zenith angle. Some small biases were produced by the AFGWC polynomials. This bias was eliminated by always making the zero order coefficient equal to 1. The new polynomials (with no bias) and the corrected channel F8 polynomial (equal to F1) are shown in Figure 3.4. The required corrections for channels F8 and F1 show some slight differences even though the polynomials (ratios) are identical. The absolute correction is dependent on the mean values used to plot Figure 3.4. The mean value for channel F1 is larger than the mean for channel F8 (as shown in Table 3.1), therefore the required correction is similar but not identical for each channel.

These zenith angle correction polynomials are now better suited for application without biasing or adversely affecting SSH-1 statistics. However, it is suggested that any zenith angle correction be more data sample specific or be general enough to apply latitudinally and/or seasonally. The differences between the required corrections at 57° for the two data sets for some of the more transparent channels is much larger than the radiance noise level (assuming a noise level of about 0.25 $mW/(m^2 sr\ cm^{-1})$). However, the polynomials provided by AFGWC, with the improvements suggested here, do produce a required correction for channel F8 that does agree with the January 1979 data sample studied.

The suggestions made here will be applicable to SSH-2 data which is to be available in 1982. These zenith angle nomalizing procedures will continue to be required if a statistical retrieval scheme is to be applied uniformly to radiance measurements from various viewing angles.

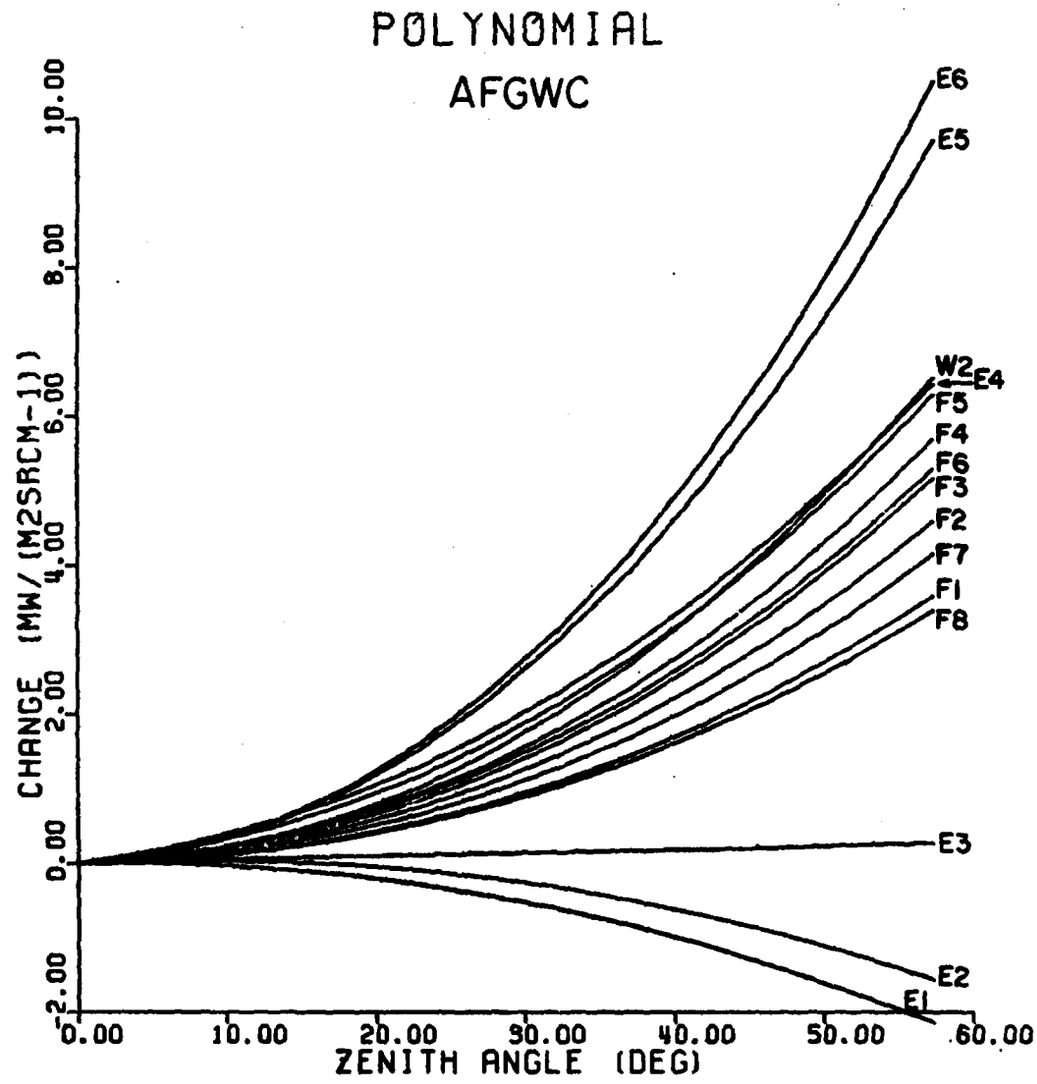

Figure 3.4. Required SSH-1 radiance change as a function of zenith angle for AFGWC polynomials with channel F8 polynomial equivalent to that of channel F1 and for no bias at zero zenith angle.

4.0 CLOUD ELIMINATION TECHNIQUES

In both the structure analysis and the scan-angle correction, it is important to eliminate the effects of clouds on the SSH-1 radiances. Clouds normally reduce the radiance by an amount which is proportional to the cloud amount, so varying amounts of cloud in adjacent FOVs cause the structure to be abnormally high. With clouds eliminated the structure should reflect only mean horizontal gradient in the atmospheric and surface parameters.

One way to eliminate clouds is to establish a minimum threshold radiance below which the FOV is assumed to contain at least a fraction of cloud. Usually this threshold is picked to correspond to a certain surface temperature. The window channel at 11 μm was used here since it is the most transparent to the atmosphere and most affected by clouds. In the case of the mid-latitude area under study, thresholds of 75, 80, and 85 $mW/(m^2 sr\ cm^{-1})$ were chosen. These correspond to surface temperatures of approximately -8°, -4°, and $0^{\circ}C$. These thresholds were tested experimentally and the exact value used should depend on the expected background (surface) temperature. For the mid-latitude region with measurements taken in November the lowest threshold, corresponding to $-8^{\circ}C$, seems to be optimal, whereas much higher threshold temperatures were used for the subtropic region (typically 0 or $10^{\circ}C$). Surfaces colder than the threshold probably contain at least a small fraction of cloud, causing the observed radiance to correspond to a lower equivalent temperature than the actual surface temperature.

A second cloud detection approach was also used. This method relied on the two measurements made using the window channel filter. (Each SSH-1 radiance channel is sensed twice for each FOV). This method is a variation of the technique to determine surface temperature and cloud amount using two window channels in different spectral regions (Smith and Rao, 1973), which will be discussed in the next subsection.

Using the two looks through the window filter it was thought that any slight shift in the FOV or change in cloud characteristics (if possible) would be reflected in a changing window radiance. The two looks would give slightly different radiances since the observed cloud field for one look would be slightly different than for the other look. This method was used to eliminate FOVs with normally high radiances, above the minimum threshold, but which possibly contained small cloud amounts. The only confirmation, however, was that this method seemed to eliminate those spots which had lower (and possibly cloudy) radiances when compared to adjacent scan spots. The structure values became more well behaved once this detection method was in effect, in that much small scale variability seemed to be eliminated, and the curves fit to the 1-dimensional structure values produced more realistic noise levels.

In the case of the two window looks, the radiance for one look is given in data provided by AFGWC, and the mean radiance for the two looks is also given, so the difference between one look and the mean would be half that between the two measurements. This is just mentioned because it is thought it would be better to have both measured values rather than one value and the mean since the difference is normally not very large, usually on the order of 0.5 mW/(m^2sr cm^{-1}) or less. Radiance difference thresholds of 0.1 or 0.2 mW/(m^2sr cm^{-1}), therefore, seemed to

eliminate most small scale noise.

A number of different combinations of the two thresholds (minimum value and difference) were used in the structure analysis provided in the previous sections. For example, the structure values in Figure 2.2 were calculated using window channel thresholds of 100 mW/(m^2sr cm^{-1}) minimum and 0.1 mW/(m^2sr cm^{-1}) difference. The noise level results (extrapolations) were dependent on the thresholds chosen. A number of noise levels were then generated and the most probable value was chosen when that value was obtained using different threshold combinations. Usually the tighter thresholds (higher minimum window radiances and lower window difference) produced more reasonable noise results. The lower noise level was chosen in cases where an alternate but higher noise level seemed unreasonable.

4.1 Single FOV Cloud Determination Using Two Window Channels

By using coincident measurements from two window channels with different spectral responses we can effectively split a single Field-of-View (FOV) into a clear sub-area and an adjacent cloudy sub-area each with a different temperature. This capability is due to the different spectral responses of each channel. Various assumptions must be made about the FOV and the window channels. The first assumption is that only two separate sub-areas comprise the total FOV (i.e. the surface and cloud sub-areas are uniform). A second assumption is that the differing measurements between window channels are more a result of spacial variations in the viewed temperature field than of any atmospheric absorption differences between the two window channel values. The equation governing either of these window channels is then:

$$B(T_{eff,i},k_i) = (1-\rho)\ B(T_{sfc},k_i) + \rho\ B(T_{cld},k_i)\quad i = 1,2 \qquad (4.1)$$

where B is the Planck function, k_i is the channel wavenumber, and the FOV is split into a clear and cloudy fraction with ρ equal to the cloud amount. As their name implies, these window channels encounter little atmospheric absorption. Therefore, the two terms in the equation originate from the surface and cloud fractions, respectively, with no atmospheric contribution.

If two window channels such as 3.7 and 11 μm are used to view such a split FOV, then the individual spectral responses of the channels will cause each to give a different effective temperature, T_{eff}. This is due to the non-linear resonse of the Plank function with respect to temperature variations. On the other hand, a uniform FOV would give the same effective temperature in both channels. For example, a uniform 0°C (273 K) FOV will give radiances of 0.18 and 76.5 mW/(m^2sr cm^{-1}) at 3.7 and 11.1 μm, respectively. However, a FOV which is partially cloud contaminated would give lower radiances and lower effective temperatures in both channels. The channel affected most would be the longwave (11.1 μm) channel. The warm (surface) fraction of the FOV would effectively contribute more to the 3.7 μm radiance than the 11.1 μm radiance although both channels see the same FOV and therefore the same cloud amount.

The use of the two window channels for cloud determination is not without precedence. Smith and Rao (1973) dealt with the 3.7 and 11 μm window channels as applied to two adjacent FOVs. They solve four equations with four unknowns: the surface temperature, the cloud temperature, and the cloud amount in each FOV. To solve this set of

equations they asume that the average surface and cloud temperatures are the same for the two FOVs.

Dozier (1980), and Matson and Dozier (1981), however, dealt with the same window channels using only one FOV by assuming that we know or can assume the surface temperature, T_{sfc}. This requires only two equations to be solved for the cloud temperature T_{cld} and cloud amount ρ. The solution is dependent on the assumed surface temperature, but the solution is unique. The noise on the radiances, however, may place the solution outside of physically reasonable limits.

By eliminating the cloud amount ρ from the two Equations 4.1 we get:

$$A_1 \cdot B(T_{cld},k_1) + A_2 \cdot B(T_{cld},k_2) + A_3 = 0 \qquad (4.2)$$

where A_1, A_2 and A_3 are known if the surface temperature is assumed,

$$A_1 = B_{sfc,2} - B_{eff,2}$$

$$A_2 = B_{eff,1} - B_{sfc,1}$$

$$A_3 = B_{eff,2} \cdot B_{sfc,1} - B_{eff,1} \cdot B_{sfc,2}$$

and

$$B_{sfc,i} = B(T_{sfc},k_i)$$

$$B_{eff,i} = B(T_{eff,i},k_i)$$

The effecitve temperature T_{eff} in each channel is a known measurement, as well as the channel wavenumber k_i.

Equation 4.2 cannot be solved explicitly since it is nonlinear in temperature. An iterative solution is simple if a starting cloud

temperature is assumed. A simple starting assumption would be

$$T_{cld} < T_{11} < T_{3.7} < T_{sfc} \tag{4.3}$$

After the cloud temperature is found, the cloud fraction is determined by solving for ρ from the original two equations, one for each channel

$$\rho = \frac{A_3}{A_4} \tag{4.4}$$

where

$$A_4 = B_{cld,2} \cdot B_{sfc,1} - B_{cld,1} \cdot B_{sfc,2} \tag{4.5}$$

and

$$B_{cld,i} = B(T_{cld}, k_i) \tag{4.6}$$

If there were equal signs in Equation 4.3 the cloud amount ρ either equals 0 or 1. These limiting cases yield a result involving no distinction between the two window channels (i.e. a FOV comprised of only a single effective temperature, either totally clear or totally cloudy).

The assumption of little or no atmospheric contribution for the window channels can be overcome by correcting the window channels for any atmospheric absorption which might occur. This can be done by using assumed atmospheric temperature and moisture profiles to estimate the atmospheric transmittance in each channel.

The radiative transfer equation (RTE)

$$L(T_i, k_i) = B(T_{eff}, k_i)\ \tau_i(T(p), Q(p)) + \sum_p B(T(p), k_i)\ \frac{d\tau_i}{dp}\, dp \tag{4.7}$$

can be solved for the effective temperature $T_{eff,i}$ given the equivalent brightness temperature T_i. The transmittance τ_i for each channel is calculated from the assumed temperature and moisture profiles T(p), Q(p). These atmospheric corrections are small in most cases, typically 1 to 2 K for a relatively dry atmosphere.

Another necessary correction would be for reflected radiation in the shortwave (3.7 μm) channel. This correction can be on the order of 10 K for 50% cloud cover. (See Hayden, et al (1981) for details). This reflected correction should be applied before any atmospheric correction is made.

This single FOV technique has been tested on some TIROS Operational Vertical Sounder (TOVS) radiances from the TIROS-N and NOAA-6 satellites. Figure 4.1 shows the window brightness temperature difference as a function of the satellite-derived bi-directional reflectance. The high correlation of 0.89 for this data signals a strong relationship and the ability of the two window channels to detect clouds based on their difference. The same techniques can be applied to the SSH-2 instrument which will contain both 3.7 and 11 μm window channels. Cloud temperature (or cloud height) and cloud amount can therefore be determined for a single FOV. Uncertainty in the radiances and the corrections to the radiances will cause some non-physical solutions (i.e. $\rho < 0$ or $\rho < 1$). These, however, can be handled as limiting cases $\rho = 0$ or $\rho = 1$ within the bounds of the uncertainty in the measurements and assumptions.

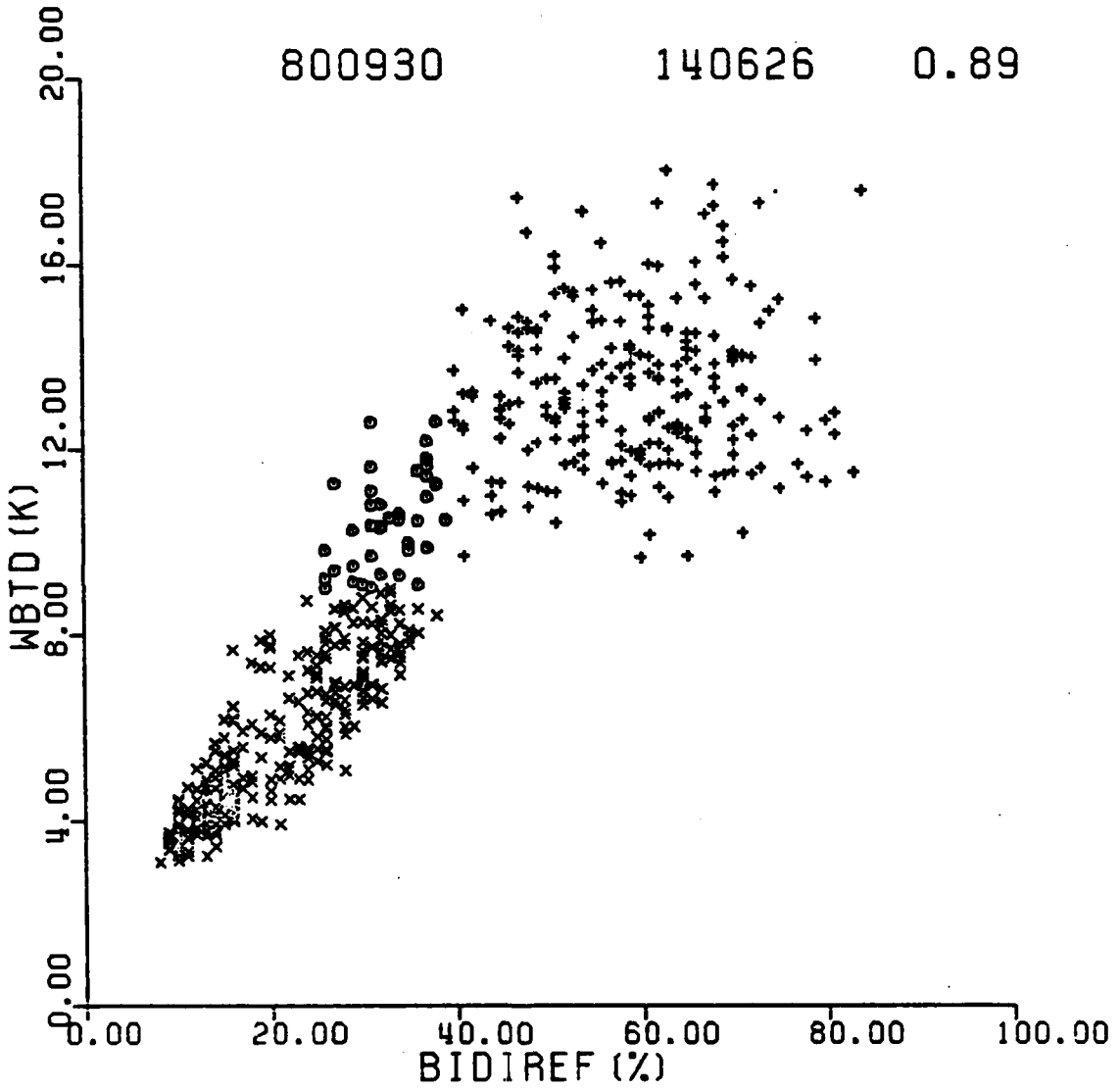

Figure 4.1. The window brightness temperature difference (WBTD) as a function of the satellite-derived bi-directional reflectance for NOAA-6 HIRS-2 window channels at 3.7 and 11 μm. A correlation coefficient of 0.89 is given.

5.0 STATISTICAL RETRIEVAL ASSESSMENT

The main thrust here was to test a statistical eigenvector retrieval technique such as used at AFGWC for SSH-1 retrievals. This algorithm was compared to simple regression to determine the maximum retrieval capabilities on the dependent data set. An independent (test) data set would give larger 'errors'. The 'errors' here are differences between RAOB temperature and moisture values and those retrieved at nearby satellite soundings. It should also be noted that the 'errors' mentioned in this section include errors in the RAOBs and differences in the time and spatial coverage of satellite soundings versus RAOBs. Differences in time of up to $\pm$ 3 hours were allowed, as were differences of up to 100 nautical miles (185 km) in location of the RAOB versus the scan spot center. The statistical data base acquired from AFGWC contained 542 such pairs which composed the data set used in this study. All regions of the globe are covered, but the soundings are weighted heavily towards the northern hemisphere.

In an effort to determine the maximum accuracy at which temperatures and mixing ratios can be retrieved from the SSH-1 data, two computer programs were written to do statistical retrievals. The first does retrievals by multiple linear regression. It works as follows. Let $\underset{\sim}{t}$ be a vector of 15 temperature deviations from the mean at the 15 standard levels from 10 to 100 mb and $\underset{\sim}{t}_B$ be a vector of 15 brightness temperature deviations from the mean for the 6 CO_2, 8 H_2O, and one window channel on the SSH-1. Then we want to find a matrix C which

relates the two in the manner:

$$\underset{\sim}{t} = C\underset{\sim}{t}_B \tag{5.1}$$

The matrix C is found by the least-squares method, that is, by forming the matrices of T and T_B whose columns are the $\underset{\sim}{t}$ and $\underset{\sim}{t}_B$ vectors respectively from the paired radiance-RAOB data. The best fit C is then

$$C = TT_B^T(T_BT_B^T)^{-1} \tag{5.2}$$

where the superscript T indicates transpose, and the superscript -1 indicates the inverse. Regression of mixing ratio was done similarly, but with values of mixing ratio in $\underset{\sim}{t}$ vectors of length 6.

For the first experiment, matrix C was calculated for data between 30°N and 60°N (mid-latitude) and for dates between 26 June 1979 and 2 February 1980, which included 118 of the 542 satellite-RAOB pairs. (No descrimination was made for the data from different SSH-1 instruments on different satellites). Errors in the regression equation using this dependent data were then calculated. This error is an estimate of the best that the SSH-1 instrument is able to do at retrieving atmospheric parameters. Figure 5.1 shows the temperature errors, and Figure 5.2 shows the mixing ratio errors. In the process of calculating the mixing ratios some extremely large values were found. Figure 5.2 was calculated after mixing ratios greater than the mean plus three standard deviations were removed from the sample. These large mixing ratios may or may not be in error, but in estimating the best that the sounder could do it seemed appropriate to throw out the large data.

As can be seen in Figure 5.1 an SSH-1 instrument can do a fairly

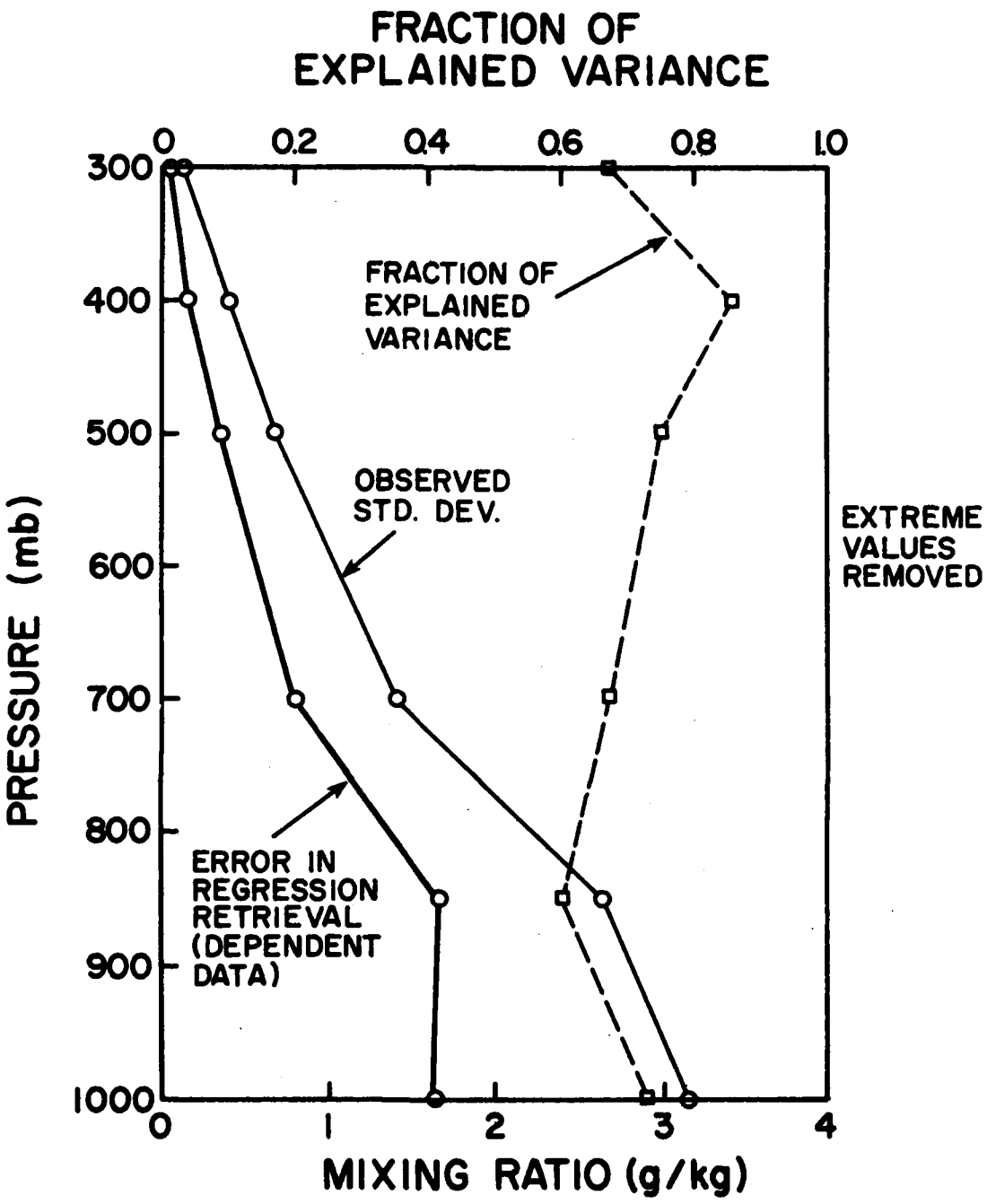

Figure 5.2. Root-mean-square mixing ratio error as a function of pressure for the SSH-1 regression retrieval on the same (dependent) data set used to develop the regression coefficients.

good job of estimating temperatures. Correlation coefficients between retrieved temperatures and RAOB temperatures are 0.9 or above except near the tropopause (200 - 300 mb). Absolute errors are less than 3 K rms in the middle troposphere (700 - 300 mb) and in the stratosphere (10 - 150 mb). Correlation coefficients between retrieved and observed mixing ratios are not as high as for temperatures, and the error at low levels is 1 - 2 g/kg. If this technique were tested on data other than that used to develop the regression coefficients (independent data), the results would be worse overall, and we suspect they would be significantly worse for the mixing ratios.

The second retrieval program tested does retrievals by the Smith-Woolf eigenvector technique (Smith and Woolf, 1976). The purpose of this was to find any errors in the eigenvector technique which is in operational use at AFGWC. If the number of eigenvectors used in the solution is equal to the number of brightness temperatures (channels) then the eigenvector technique is identical to the regression technique. If fewer eigenvectors are used to determine the C matrix, the error is increased for dependent data. (The eigenvector technique can actually outperform the regression technique on independent data). Shown in Figures 5.3 and 5.4 are the mass-weighted average rms errors in retrieving temperatures and mixing ratios, respectively, versus the number of eigenvectors used to determine the C matrix. Shown for comparison is the mass-weighted average rms error for the regression technique.

The maximum possible number of eigenvectors which can be used to construct the C matrix is the lessor of the number of levels to be retrieved and the number of channels used in the retrieval — 15 for

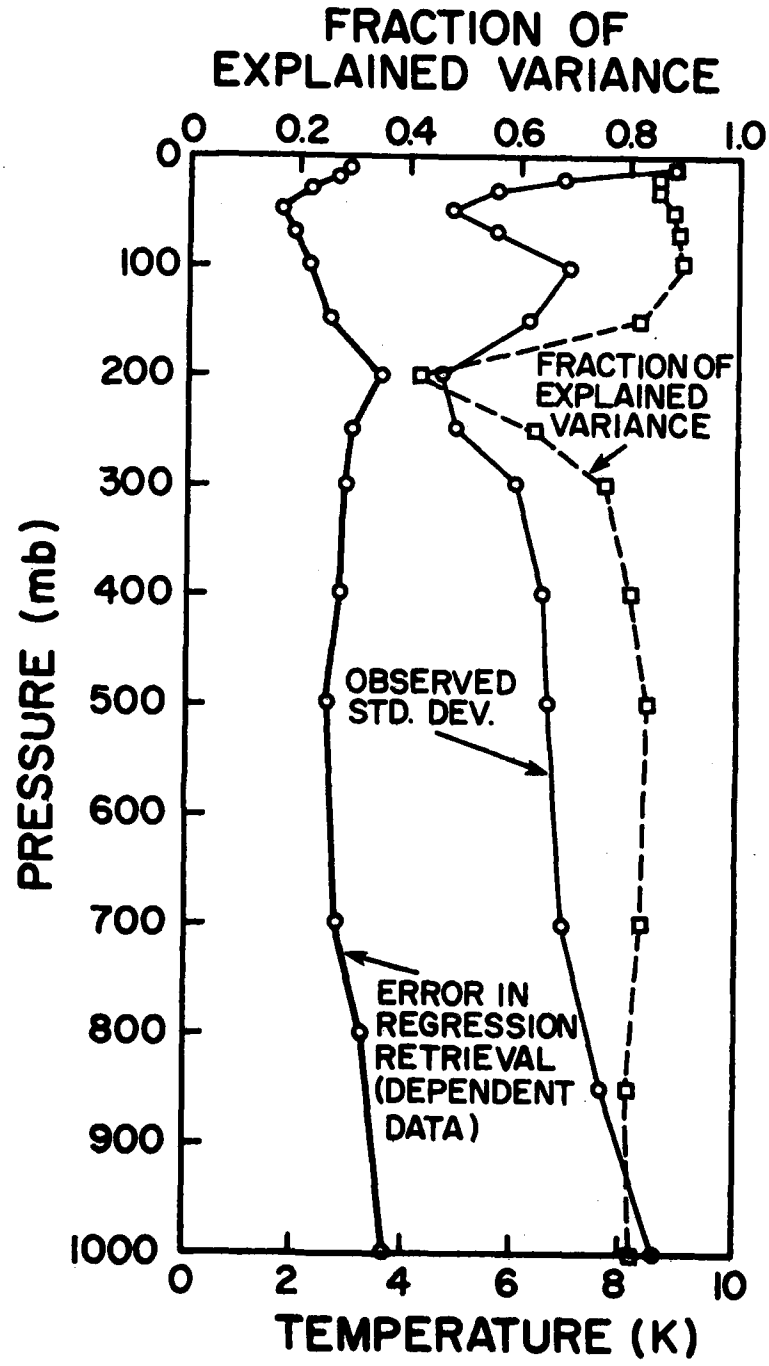

Figure 5.1. Root-mean-square temperature error as a function of pressure for the SSH-1 regression retrieval on the same (dependent) data set used to develop the regression coefficients.

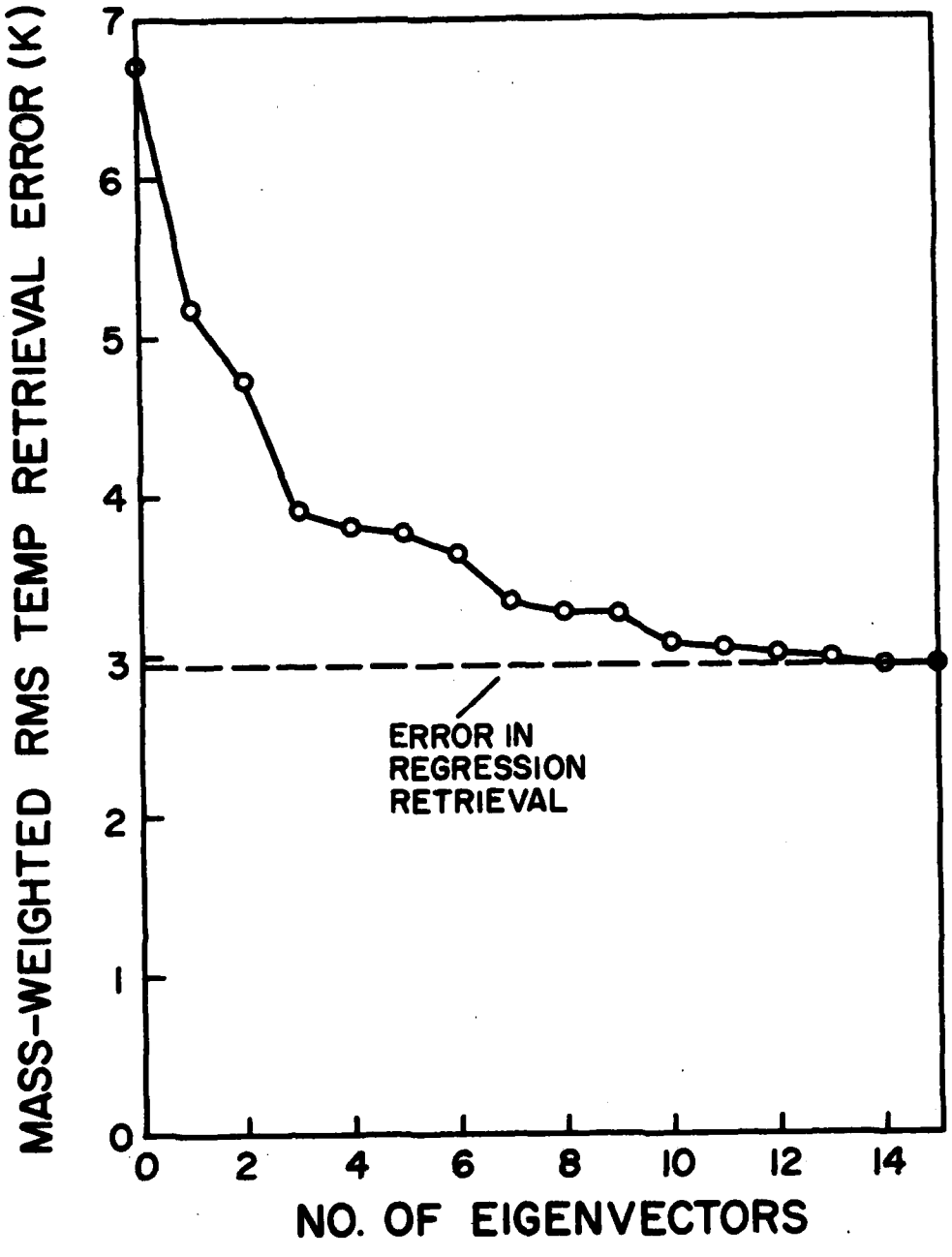

Figure 5.3. Mass-weighted average rms temperature error as a function of the number of eigenvectors used in the SSH-1 eigenvector retrieval.

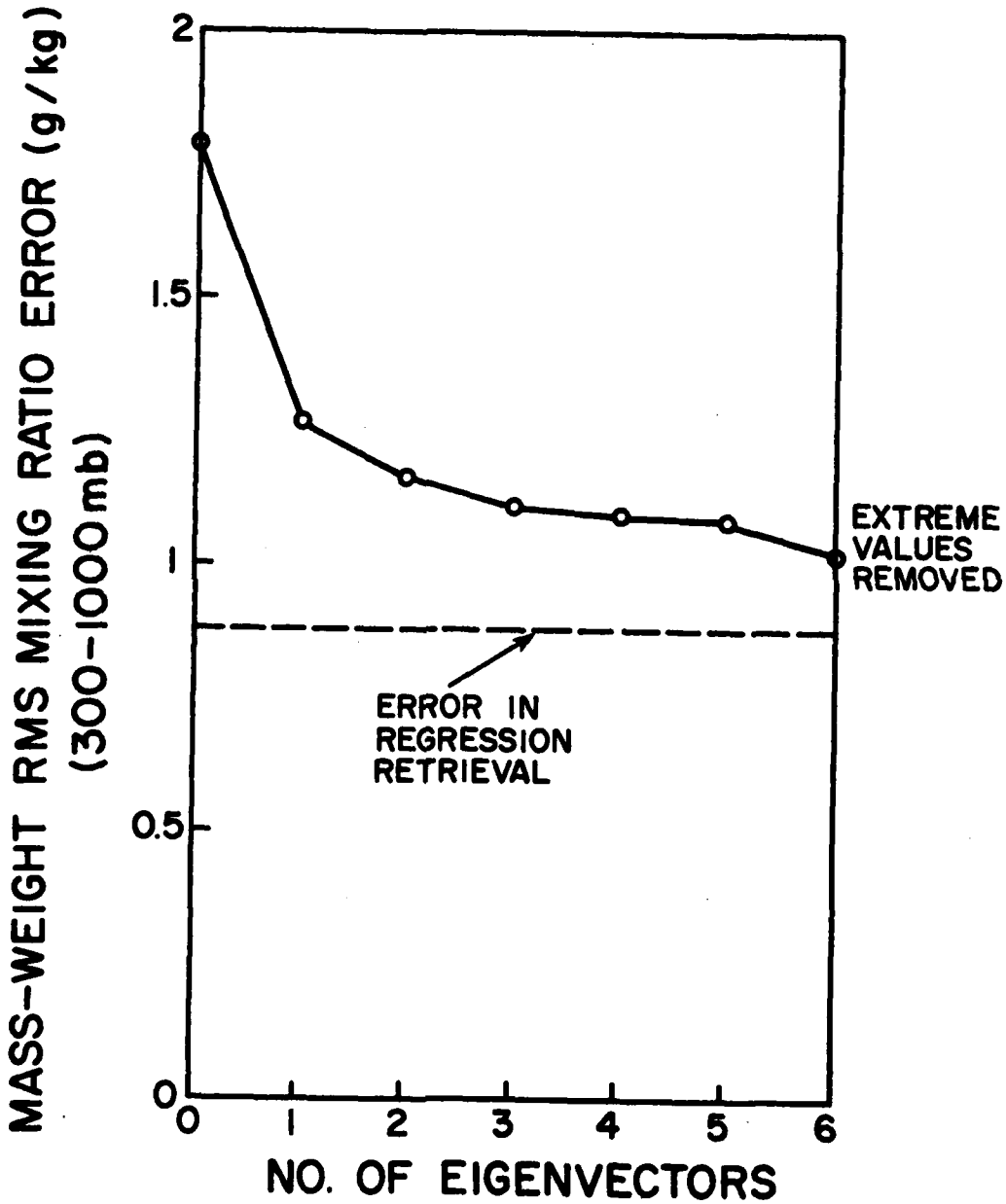

Figure 5.4. Mass-weighted average rms mixing ratio error as a function of the number of eigenvectors used in the SSH-1 eigenvector retrieval.

temperatures, 6 for mixing ratios. Figures 5.3 and 5.4 show that using about half of the maximum number of eigenvectors (7 for temperatures, 3 for mixing ratios) reduces the 'error' by 90% of the potential reduction.

These moisture results compare favorably with previous tests of the accuracy of retrievals using the SSH-1 radiances (Klein et al, 1976; Wachtmann et al, 1974; Mount et al, 1977) which show rms temperature 'errors' of 2 to 4 K as typical. However, the larger 'errors' in retrieval of moisture parameters at AFGWC are most likely not caused by the retrieval programs used, but are probably a function of the statistical radiance-RAOB sample or of the independent data sets under study. Some large moisture variances were found in the RAOB data and these could adversely affect the retrieval results.

If statistical retrieval schemes continue to be used, then the radiance-RAOB pairing should be better scrutinized to eliminate suspected noise in both the radiances and the conventional soundings. This is critical to the statistical retrieval scheme in both the production and use of the C matrix. Communication with personnel at AFGWC confirmed that such problems have existed and should be corrected if reasonable moisture results are to be obtained. It is also suggested that the temperature and moisture retrievals be conducted separately in order to avoid contaminating the retrieved temperatures with noise from the moisture channel radiances and vice versa.

5.1 Regression Error Analysis on Independent Data Sets

Regression retrievals were also performed on independent data sets (data sets other than those used to develop the regression equations). The errors for retrievals using independent data should increase above

those for retrievals using dependent data sets. In this application alternate retrieval schemes can make improvements over simple regression retrievals. An eigenvalue/vector retrieval scheme, for example, can actually out-perform the regression retrievals on independent data. This is done by eliminating some high-order eigenvectors which carry only noise information.

The independent-set regression experiments were conducted using all 542 souning pairs provided by AFGWC. To determine the minimum error levels obtainable with this larger set of data, the satellite-RAOB pairs were first used both to develop the regression equations and then as a dependent set to test the regression retrieval scheme. Alternately, to provide both a dependent and an independent data set, the 542 satellite-RAOB pairs were split various ways into two equal size sets. Four methods were used to make this division. Each case allowed half of the of the set (271 satellite-RAOB pairs) to be the dependent set for development of the regression coefficients and the other half to be the independent set for testing of the regression equations. The divisions were:

1) odd pairs as dependent set, even pairs as independent set;
2) even pairs as dependent set, odd pairs as independent set;
3) first half as dependent set, second half as independent set;
4) second half as dependent set, first half as independent set.

The results using each of the 4 divisions of the satellite-RAOB data were then averaged to give representative 'errors' for a regression retrieval scheme on data other than that used to derive the regression coefficients. The results are given in Tables 5.1 and 5.2 which show the temperature and mixing ratio errors respectively. Some of the

Table 5.1

Temperature Regression Errors for 542 Non-Cloudy Satellite-RAOB Pairs (June 1979 - February 1980)

Level (kPa)	Sample Std. Dev. (K)	Temperature Error (K) All Dependent	Expl. Var.	Odd-Even	Even-Odd	First-Second	Second-First	Half-Half Mean	Expl. Var.
1	15.6	3.7	(.94)	4.0	3.9	3.7	4.0	3.9	(.94)
2	13.0	2.7	(.96)	3.1	3.1	2.9	3.3	3.1	(.94)
3	11.4	2.1	(.96)	2.2	2.4	2.2	2.4	2.3	(.96)
5	10.0	2.0	(.96)	2.3	2.1	2.2	2.5	2.3	(.95)
7	9.0	2.1	(.95)	2.0	2.2	2.2	2.4	2.2	(.94)
10	8.0	2.0	(.94)	2.1	2.2	2.1	2.3	2.2	(.93)
15	7.2	2.0	(.92)	2.1	2.1	2.0	2.6	2.2	(.90)
20	7.2	3.1	(.82)	4.6	3.0	3.3	6.1	4.3	(.60)
25	6.2	3.4	(.70)	5.2	3.6	3.6	5.8	4.6	(.56)
30	7.4	3.4	(.79)	5.1	3.6	3.6	6.6	4.7	(.55)
40	9.2	3.5	(.85)	4.5	3.8	3.9	6.2	4.6	(.74)
50	10.0	3.6	(.87)	4.5	3.8	4.0	6.0	4.6	(.78)
70	10.8	3.7	(.88)	4.0	3.8	4.1	4.1	4.0	(.86)
85	11.7	3.9	(.89)	4.4	4.0	4.2	4.1	4.2	(.87)
100	14.7	4.0	(.93)	4.2	4.0	4.2	4.2	4.3	(.92)

Table 5.2

Mixing Ratio Regression Errors for 542 Non-Cloudy Satellite-RAOB Pairs (June 1979 - February 1980)

Level (kPa)	Sample Std. Dev. (g/kg)	Mixing Ratio Error (g/kg) All Dependent	Expl. Var.	Odd-Even	Even-Odd	First-Second	Second-First	Half-Half Mean	Expl. Var.
30	.072	.05	(.46)	.05	.06	.05	.06	.06	(.42)
40	.254	.08	(.51)	.18	.21	.17	.20	.19	(.42)
50	.486	.35	(.48)	.44	.42	.35	.41	.40	(.36)
70	1.24	.84	(.54)	1.15	.92	.90	1.09	1.02	(.31)
85	2.06	1.26	(.63)	1.52	1.38	1.33	1.53	1.44	(.50)
100	2.81	1.34	(.77)	1.61	1.46	1.33	1.53	1.48	(.72)

tabulated results are also plotted in Figures 5.5 and 5.6. The standard deviations (square root of total variance) of the meteorological parameters at various levels are also given. These standard deviations show the variability of the data and can be used as a baseline for understanding the noise levels. The explained variance values:

$$\text{Expl. Var.} = 1 - \frac{\text{error variance}}{\text{total variance}} \tag{5.3}$$

give a measure of the amount of variance of the whole data set that can be explained by the regression retrieval scheme. This value will range from 0 to 1, with zero indicating that the retrievals explain none of the data variability (i.e. the error variance is as large as the variance of the total data set). An explained variance value approaching 1 would indicate an error variance much smaller than the variance of the total data set, or good satellite retrievals when compared to RAOBs.

The results in the first four columns of Table 5.1 show that the temperature errors reach a minimum of about 2 K rms in the lower stratosphere. The sample standard deviation, however, is also low here, but the explained variance is still very high. Temperature errors increase to 4 K rms at the surface and also increase at higher levels. The minimum explained variance of 70% occurs at the 25 kPa (250 mb) level, near the tropopause.

The error statistics for the various half dependent-half independent data set divisions are also shown as well as the half dependent-half independent mean errors. These errors increase slightly over the totally dependent sample errors and range from 2 K in the stratosphere to 4.7 K at 30 kPa, with errors above 4 K down to the

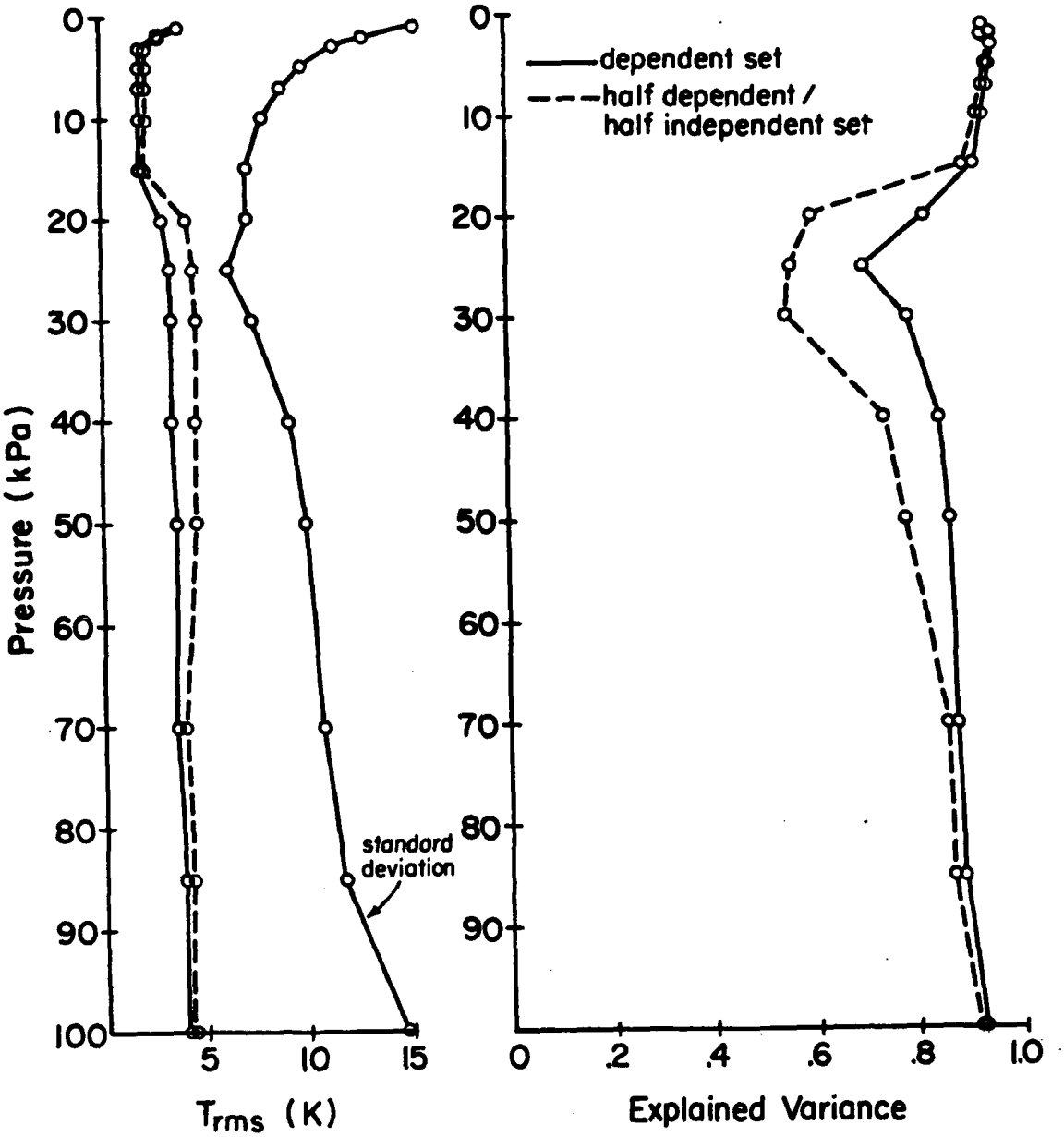

Figure 5.5. Root-mean-square temperature error as a function of pressure for SSH-1 regression retrievals on both dependent and independent (test) data sets.

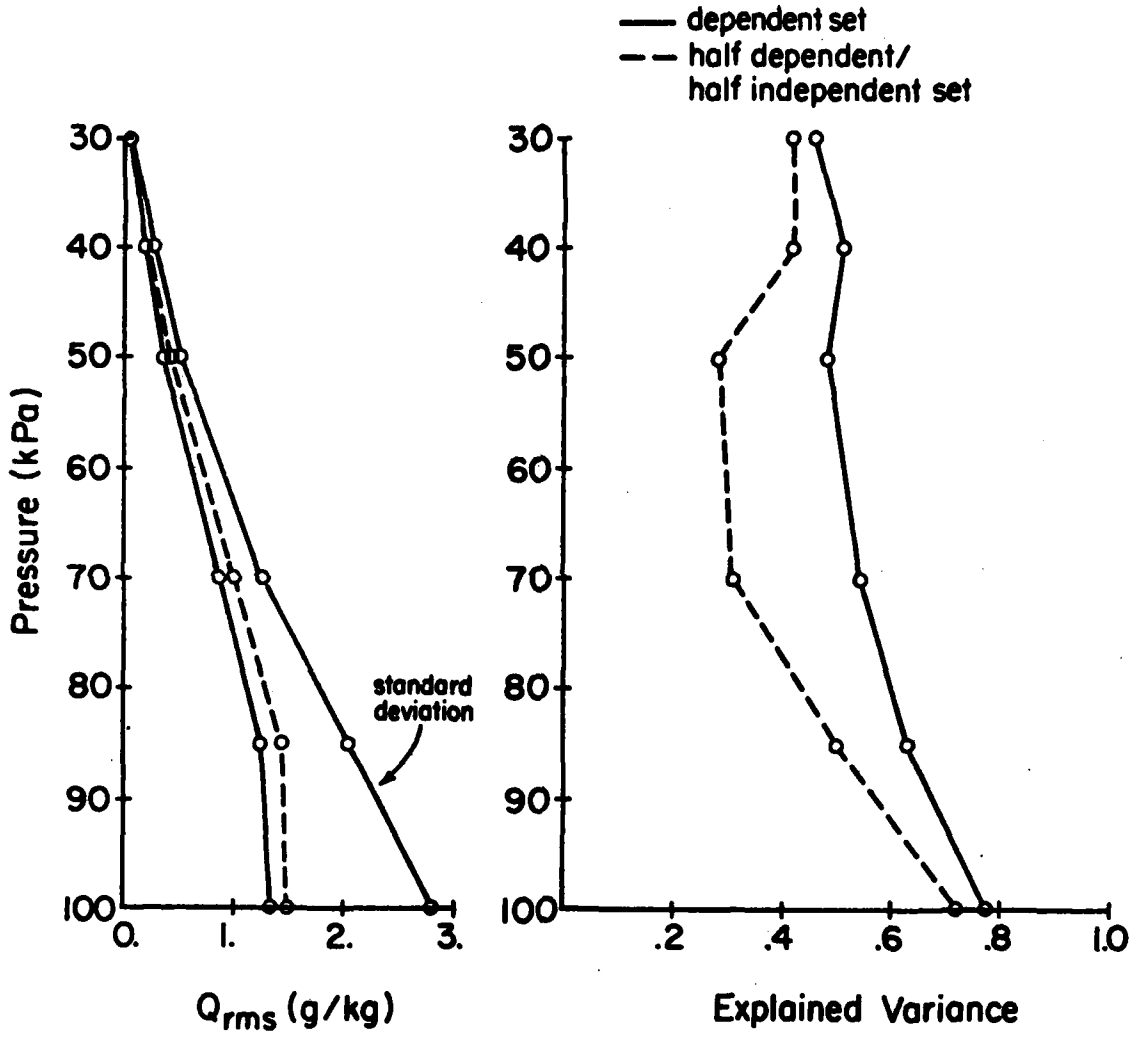

Figure 5.6. Root-mean-square mixing ratio error as a function of pressure for SSH-1 regression retrievals on both dependent and independent (test) data sets.

surface. These larger errors, however, still explain at least 55% of total variance at 30 kPa and larger amounts at other levels.

These temperature error results compare favorably with previous tests of the accuracy of retrievals using the SSH radiances (Mount, et al., 1977; Klein, et al., 1976) which show rms errors of 2 to 4 K as typical. In order to prove more effective than simple regression, any retrieval scheme developed will have to provide reduced 'errors' in a similar satellite-RAOB comparisons.

The mixing ratio errors for the 6 standard levels are shown in Table 5.2, in a format similar to Table 5.1. Because moisture resides most heavily in the lowest layers of the atmosphere the 'errors' can be expected to decrease with height. The explained variance, therefore, serves especially well to compare the 'error' to the sample standard deviation at each level, putting the 'error' in perspective. Columns 3 and 4 give the all dependent sample results, where it can be seen that mixing ratio errors increase to 1.34 g/kg at the surface. Explained variances at all levels are above 46% with the largest value of 77% at the surface. For the half dependent-half independent case the mean errors increase to 1.48 g/kg at the surface. Explained variances here range from 31 to 72%, again with the largest percentage explained variance at the surface. This is most likely due to the larger moisture signal-to-noise ratio at the surface. While the mixing ratio error decreases slightly with height, it does not decrease with height nearly as rapidly as the sample standard deviation.

The moisture results in general show a reasonable but limited moisture retrieval capability. Explained variances below 50% show very little usable information. The best moisture information therefore

comes from near the surface. Similar explained variances were determined by Savage (1980) using actual the AFGWC statistical eigenvector retrieval technique. Other moisture retults by Crane (1976) provide explained variances in total precipitable wager of slightly better than 50% using the H_2O channels only. The ability to derive moisture information was also shown to be enhanced by using actual temperature information as independent regression predictors. The explained variances then rose to the over 80% range. The use of CO_2 channel radiances directly instead of actual temperatures would degrade these results somewhat.

The results using this simple regression retrieval scheme, therefore, do confirm the results of similar studies by others. The results of course depend on the data sample under study, but with large data samples the results should be largely invariant. Any improvements to be made could possibly arise out of a more physical retrieval scheme which would better interpret the strengths of each radiance channel. An attempt at channel selection *prior* to regression retrievals is also being done in an attempt to improve the above moisture results particularly. Only with an increase in explained variance will those results be acceptable as an improvement over simple regression.

6.0 TRANSMITTANCE SOFTWARE FOR SSH-1 CHANNELS

The need for SSH-1 transmittance software arose out of a desire to implement an iterative or minimum-information retrieval scheme. These schemes do not require a history of satellite-RAOB pairs which serve as the statistical base for regression or eigenvector retrieval schemes. Instead, they require a knowledge of the atmospheric transmittances for radiation at wavelengths within the various satellite channel ranges. In an iterative retrieval scheme these transmittances can be updated with each adjustment of the temperature and moisture profiles. In a minimum-information retrieval scheme the transmittances form the basis for the retrieval matrix together with a knowledge of the noise variances.

In either retrieval scheme transmittances need to be calculated for the appropriate satellite channels. To meet this requirement, software was adapted from various sources to the SSH-1 channels. The software employed polynomial approximations of the more precise line-by-line computations. Even with the increased computation speed which results from this approximation, the software still requires significant computer resources.

6.1 H_2O and CO_2 Channels

The SSH-1 H_2O and CO_2 filter response functions obtained from AFGL were used to set up a simplified polynomial transmittance representation. The transmittances calculated by this simplified and fast method are the basis for an iterative (physical) water vapor and

temperature retrieval scheme.

Data from three sources were combined in this endeavor. Smith (1969) calculated transmittance polynomials which adequately represented the atmospheric transmittance as it was known at that time for the 15 μm CO_2 and 20 μm rotational H_2O bands. The Smith polynomials, as they will be called here, were originally developed for the SIRS (Satellite Infrared Spectrometer). The polynomial coefficients are given for every 5 cm^{-1} from about 200 to 820 cm^{-1}. These polynomials were convoluted with the SSH-1 filter response functions provided by AFGL for the H_2O and CO_2 channels. Then software developed by NOAA/NESS, similar to that used for window channel transmittance calculations (Weinreb and Hill, 1980), was modified to be compatiable with the Smith polynomials. The result was a quick and easy transmittance calculation scheme which will be explained in more detail as follows.

Smith developed a polynomial transmittance representation as a speedy alternative to the much slower (but possibly more accurate) line-by-line calculations which can be used to determine the transmittance for a given temperature and moisture profile. The polynomials provided an adequate representation of the continuum and the absorption bands as known at that time. However, improvements in transmittance measurements may have made the polynomials inadequate. This can be determined by comparison with more precise and up-to-date calculations or by comparison with emperical transmittance data.

The Smith polynomials consist of 9 terms of the form:

$$W = \sum_{i=0}^{8} C_i A_i \qquad (6.1)$$

where the C_i's are tabulated transmittance polynomial coefficients at every 5 cm^{-1} and the A_i's the polynomial terms given in Table 6.1.

Table 6.1

Smith Transmittance Polynomial Terms

Terms	H_2O		CO_2
A_0	—	1.	—
A_1	—	X	—
A_2	—	Y	—
A_3	—	Z	—
A_4	—	XY	—
A_5	—	XZ	—
A_6	—	X^2	—
A_7	X^2Z		X^2Y
A_8	YZ^2		XZ^2

where:

$$X = \ln\left[U\left(\frac{273K}{T}\right)\right]$$

$$Y = \ln\left[\frac{P}{1000mb}\right]$$

$$Z = \ln\left[\frac{T}{273K}\right]$$

The polynomial representation was derived by linearizing a transmittance approximation in terms of optical mass of water vapor or total precipitable water (U), pressure (P), and temperature (T) by taking the logarithm twice and expanding in regular polynomials such that in terms of wavenumber k:

$$\tau_{Ak} = \exp[\exp(W)] \tag{6.2}$$

The details are given by Smith (1969) or in modified form by Minnis and Cox (1976).

In order to specialize the polynomials to the sounder under study, these polynomials were convoluted with the SSH-1 H_2O ad CO_2 filter response functions. Figure 6.1 gives the filter response for channel F3 on satellite WX4537. The filter is about 30 cm^{-1} wide and is approximated every 5 cm^{-1} (where the polynomial coefficients are known) by the histogram which gives an indication of the quality of the approximation.

New polynomials were then calculated that were representations for each channel by the convolution of the tabulated polynomial coefficients with the filter response function ϕ_j for each channel.

$$D_i = \frac{\sum_{j=1}^{k} C_{ij}\,\phi_j}{\sum_{j=1}^{k} \phi_j} \tag{6.3}$$

where k is the number of Smith polynomials terms C_{ij} at 5 cm^{-1} intervals which went into the new polynomial term D_i to replace C_i in Equation 6.1. A nine-term polynomial was, therefore, derived for each channel i, which would determine its transmittance for any known pressure, temperature, and mixing ratio profile. However, for the special case of channel F5 at 536 cm^{-1} and the CO_2 channels, which experience absorption by both H_2O and CO_2, the separate H_2O and CO_2 transmittances each produced a polynomial of the form of Equation 6.1. The resulting

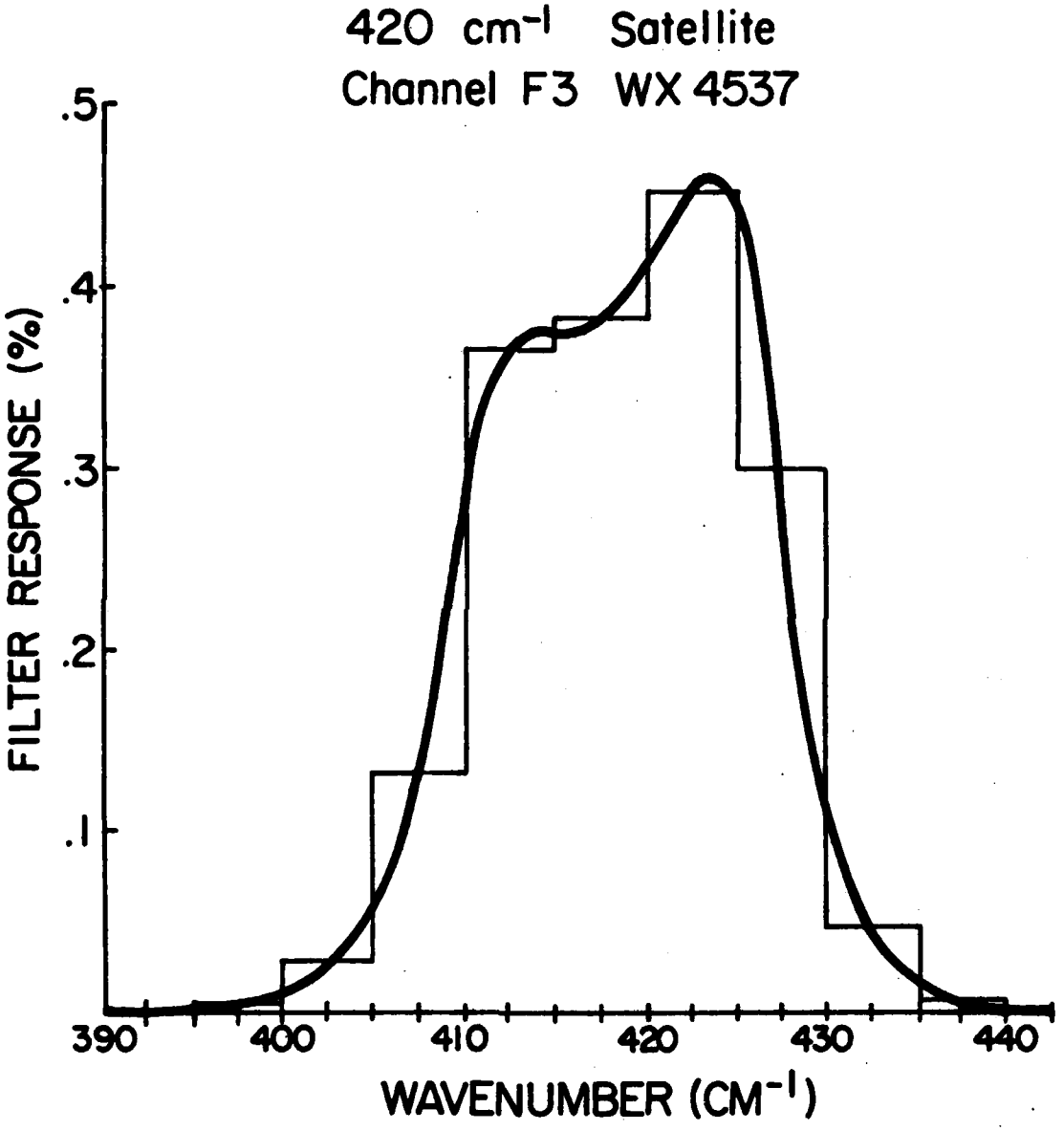

Figure 6.1. Filter response function for SSH-1 channel F3. The histogram represents the approximation over 5 cm^{-1} intervals for use with Smith transmittance polynomials.

transmittances then were multiplied together for the total transmittance.

$$\tau_{total} = \tau_{H_2O}\,\tau_{CO_2} \tag{6.4}$$

The transmittances were then numerically differenced in the vertical to produce weighting functions, as shown in Figure 6.2 for the H_2O channels. The weighting functions for all 8 H_2O channels (F1-F8) are given along with the separate H_2O and CO_2 weighting functions for the F5 channel. The weight axis units are relative to the pressure coordinate system used in the vertical differencing. These weighting functions are calculated for the 1962 US standard temperature profile and for a given moisture profile with a mixing ratio of 10g kg^{-1} at 100 kPa (1000mb) and a total precipitable water of 2.55 cm. These temperature and moisture profiles are plotted in Figures 6.3 and 6.4.

6.2 CO_2 Transmittance Problem and Solution

The first attempt at obtaining the SSH-1 CO_2 channel transmittances proved to be far from satisfactory. Many of the CO_2 channel weighting functions were remarkably similar with maximum weight well below the tropopause (typically below 500 mb). This was in strong contrast to the weighting functions for the Vertical Temperature Profile Radiometer (VTPR) CO_2 channels which have maxima spread throughout the stratosphere and troposphere (McMillin, et al., 1973). For example, the weighting function for the least transparent 15 μm channel (668 cm^{-1}) should peak well above the tropopause, as was not the case with the polynomial-approximated weighting function.

These problems lead to an evaluation of some software obtained in

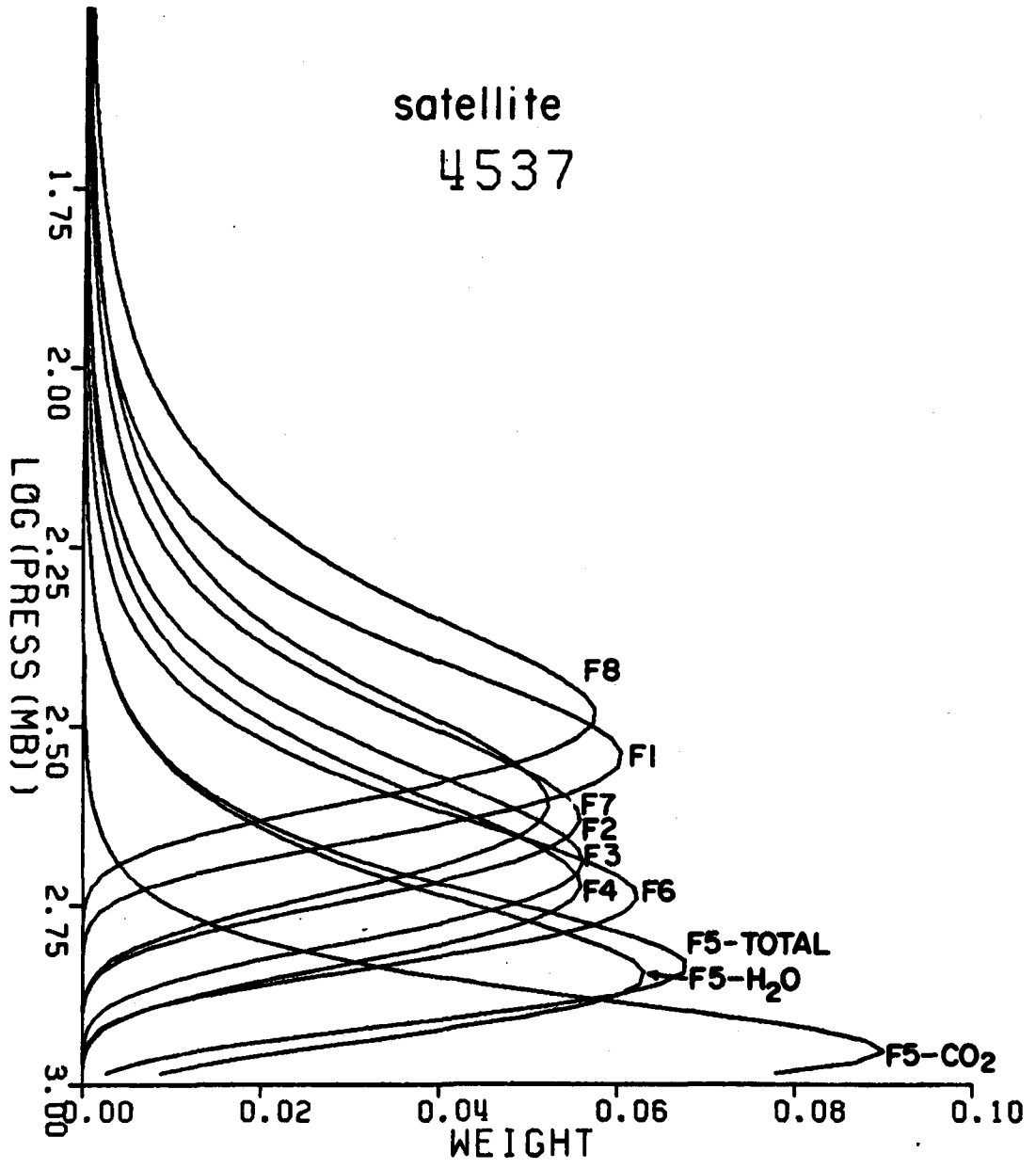

Figure 6.2. Weighting functions for the 8 SSH-1 H_2O channels (F1-F8) with separate weighting functions for the H_2O and CO_2 transmittance components of channel F5 (535^{-1}).

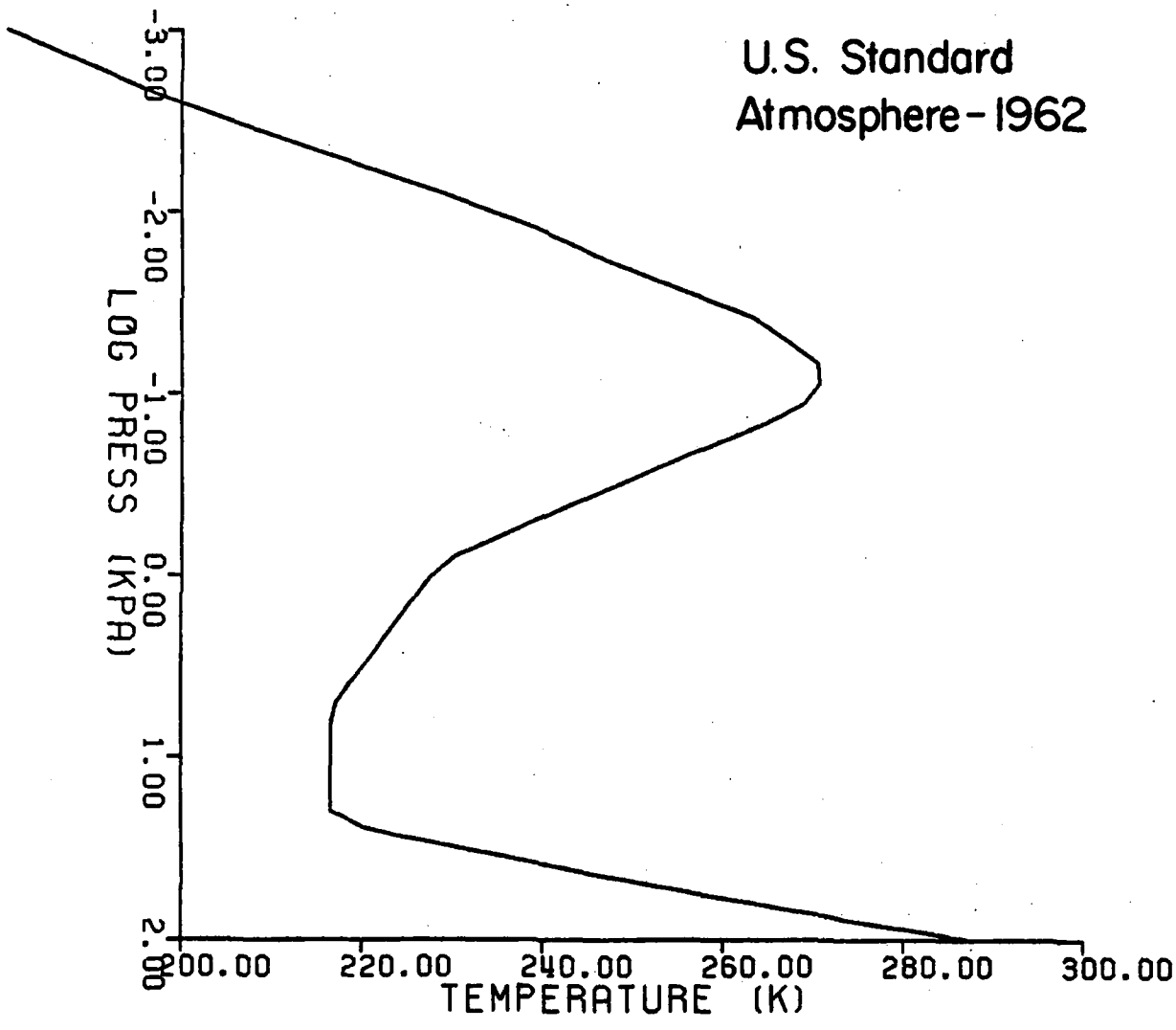

Figure 6.3. 1962 U.S. Standard Atmosphere used for transmittance calculations.

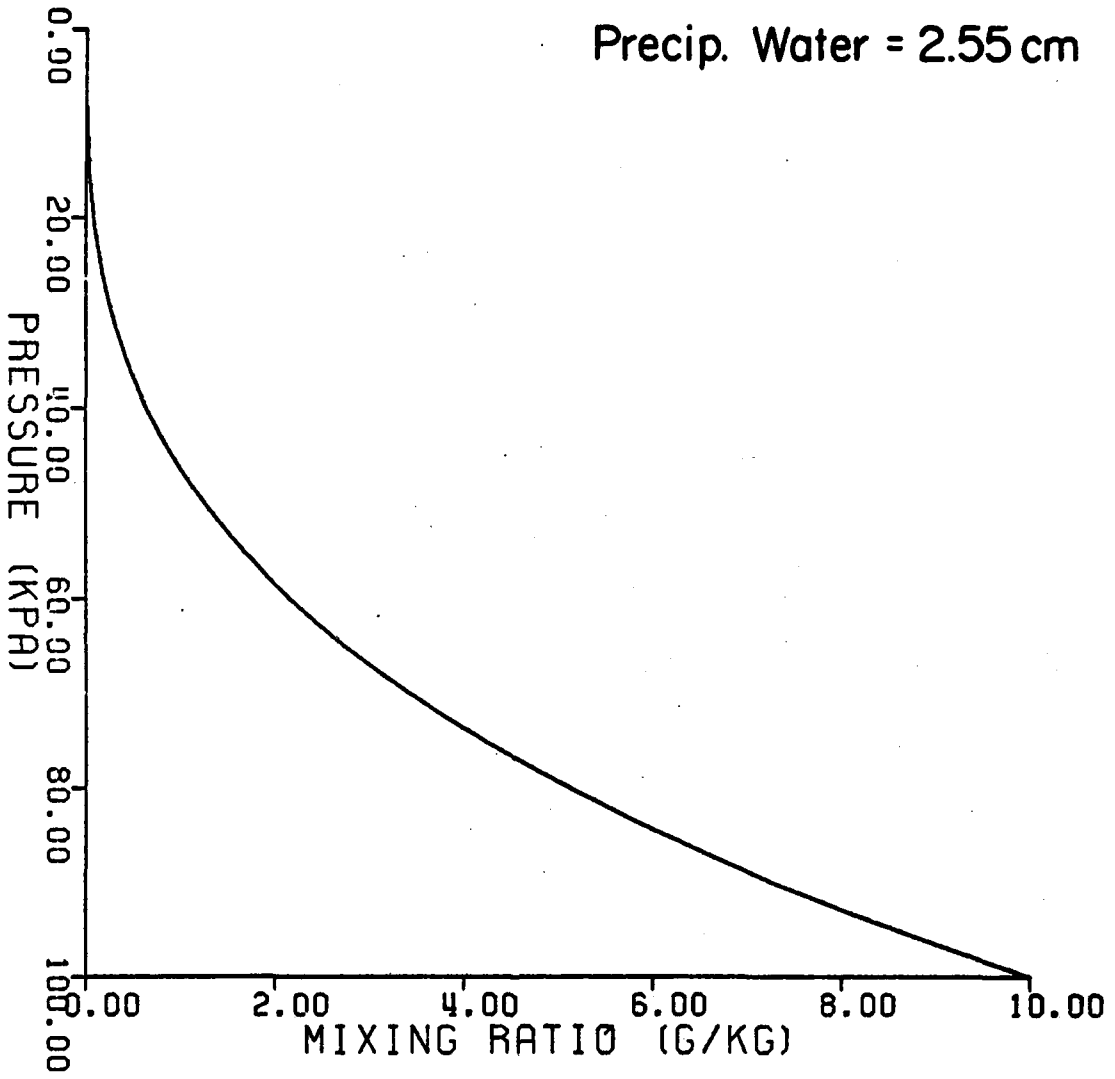

Figure 6.4. Moisture profile with 2.55 cm of precipitable water used for transmittance calculations.

1975 from NOAA/NESS for the calculation of the VTPR channel transmittances. That software was used for VTPR data from the NOAA satellite series and is based on the work of McMillin and Fleming (1976). Because of the similarity between the VTPR and SSH-1 CO_2 channels in both central wavenumber and half width the VTPR transmittance software was used as a guide in interpretng the problems with the software developed for SSH-1 and eventually as replacement software for the CO_2 channel transmittances. A comparison of the VTPR channels with the corresponding SSH-1 channels is given in Table 6.2.

Table 6.2

Comparison of VTPR and Equivalent SSH-1 Channels

	VTPR			SSH-1		
Band	Channel Number	Central Wavenumber (cm^{-1})	Half Width (cm^{-1})	Channel Number	Central Wavenumber (cm^{-1})	Half Width (cm^{-1})
CO_2	1	668.5	3.5	E1	668.5	3.5
CO_2	2	677.5	10.	E2	677.	10.
CO_2	3	695.	10.	E3	695.	10.
CO_2	4	708.8	10.	E4	708.	10.
CO_2	5	725.	10.	E5	725.	10.
CO_2	6	747.	10.	E6	747.	10.
H_2O	7	535.	18.	F5(E7)	535.	16.5
Window	8	833.	10.	W2(E8)	835.	8.

The problem with the transmittances for the SSH-1 CO_2 channels (E1-E6) seemed to stem from an incorrect application of the Smith polynomials to the CO_2 absorption in the 15 μm region. To remedy this, the CO_2 absorption part of the VTPR transmittances was adopted.

In comparison of the two sets of transmittance software another possible error was discovered. The discrepancy was a variation in the definition of the 'X' term of Table 6.1. By a comparison of the polynomials generated here for the SSH-1 channels and the polynomials

given for the VTPR H_2O absorption, a modification was made to the software to make the calculations consistent. Surprisingly the results were not affected very severly by this change.

The final CO_2 weighting functions are given in Figure 6.5. Again, these transmittances are specific to the temperature and moisture profiles used in the calculations. Before extensive use, the transmittance software should be compared to line-by-line calculations or to experimentally observed transmittances. If the transmittances are not good representations, bias errors in retrievals could result, but at least the transmittances should be known well enough in order to adequately reflect the temperature and moisture changes necessary in the retrieval process. This polynomial transmittance representation can then be used to calculate the transmittances and resulting weighting functions which are needed in a physical retrieval scheme.

6.3 Window Channel Transmittance

Finally, transmittance software based on the work of Weinreb and Hill (1980) was used for the 12 μm window channel on the SSH-1 instruments. This software was originally developed for broadband window channels on the TIROS-N/NOAA satellite series.

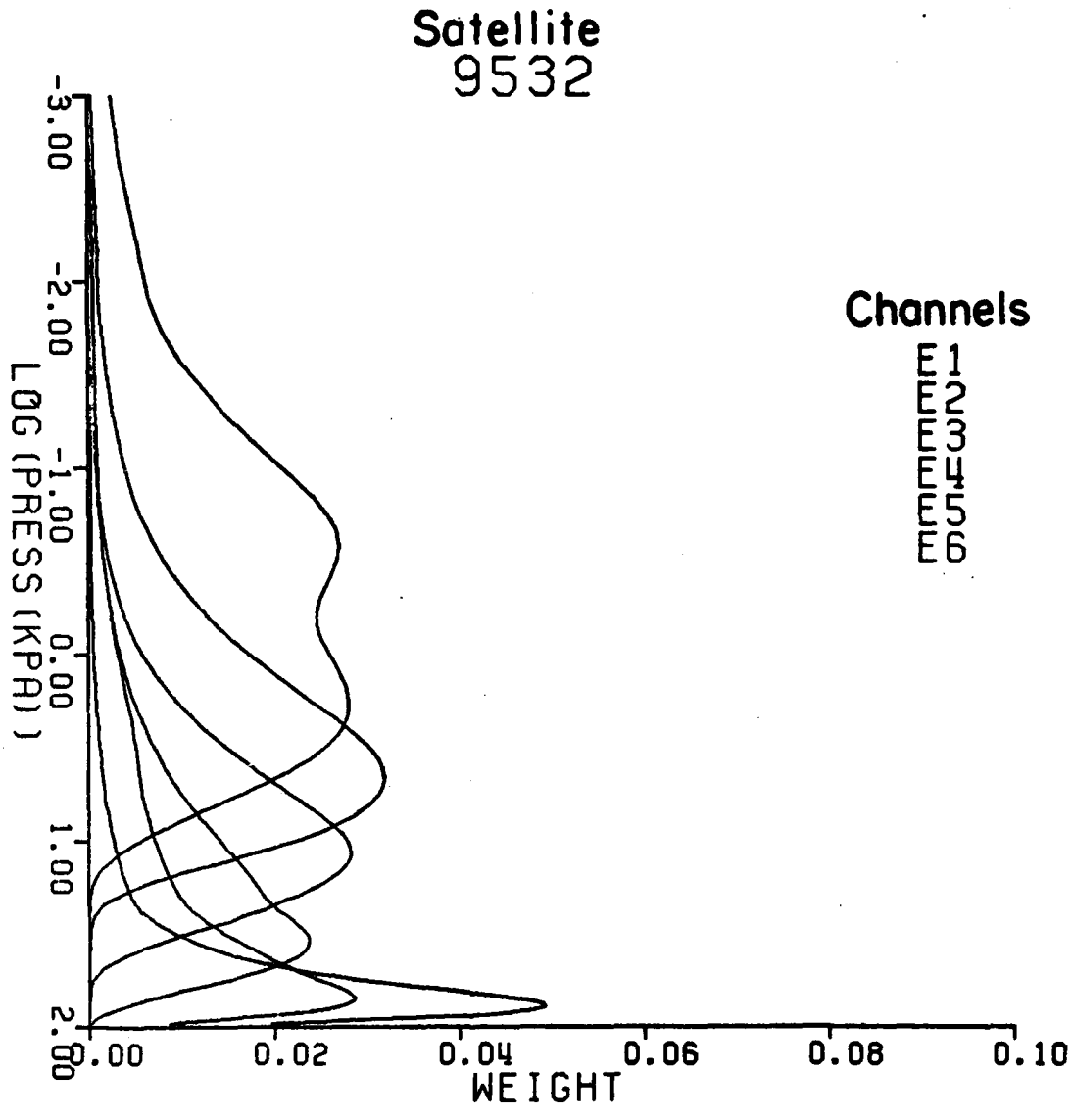

Figure 6.5. Weighting functions for SSH-1 CO_2 channels (E1-E6).

7.0 SUMMARY

Several aspects of the infrared remote sounding problem particular to SSH-1 have been addressed. Each of these areas of research is related to the two objectives listed in the introduction. For research purposes real (not simulated) SSH-1 radiance data with corresponding rawinsonde (RAOB) data were obtained from AFGWC. These SSH-1/RAOB pairs covered the period from June 1979 through February 1980.

A structure analysis was performed on the SSH-1 radiances in order to estimate the radiance noise levels. The results confirm that the SSH-1 radiances have not been degraded significantly, if at all, from their expected noise levels. (These noise levels may be translated into the uncertainty to be expected for temperature and moisture parameters provided by perfect retrieval schemes using this noisy data.) In other words, the problems with SSH-1 retrievals are not caused by noisy radiances. Eivenvector analysis, on the other hand, does indicate significant redundancy in the channels which limits the amount of information available.

The scan-angle corrections as applied by AFGWC were found to be adequate in all but one channel (F8). The solution was to apply the correction polynomial for a similar channel (F1) to the one channel (F8) for which the polynomial produced a large bias. These scan angle corrections are necessary for the application of a statistical retrieval scheme which requires radiances from a common nadir (zenith-angle corrected) viewing position.

The cloud detection problem is also very important since this is the source of many problems with infrared retrieval schemes. Small amounts of cloud as well as cirrus are very hard to detect and eliminate. Two methods are presented; one which depends on radiance thresholds which are determined emperically or theoretically; and the other method which can be applied to future SSH-2 data. The second method relies on the use of two window channels with different spectral characteristics. Both cloud amount and temperature (or height) can be determined for a single FOV if a surface or background temperature is known or assumed. This method, however, assumes that the field-of-view is only partly cloudy and contains a uniform cloud top. Even if these assumptions are not met, the two methods can effectively detect cloudy fields-of-view which can then be eliminated from consideration.

The assessment of a regression retrieval scheme for temperatures and moisture does indicate that the SSH-1 radiances do contain temperature and moisture information. Results of retrievals on independent data (data other than that used to develop the regression coefficients) are degraded from dependent data tests but are not completely noise. Moisture, especially of the lowest layers, can be retrieved, contrary to prior experience with SSH-1 data at AFGWC. These results are also confirmed by others who have worked with simulated data for SSH-1. Deficiencies in the statistical data base used by AFGWC for the regression analysis may be the source of the problem.

Finally, transmittance software for the SSH-1 H_2O, CO_2, and window channels was developed. The need for this software arose from the expected application of an iterative moisture and temperature retrieval algorithm. However, because of computing expense and time limitations

this course of research was discontinued. Much swifter regression retrievals will most likely be adopted with no degradation of retrieval quality. Appropriate selection of the SSH-2 channels which are to be used in retrieval will be necessary.

Much more work is needed, especially to obtain useful moisture information. The moisture channel radiances seem to be performing as expected, but the channel selection is far from optimized since the eigen-analysis shows that there are fewer than half as many independent pieces of information than there are SSH-1 radiance channels. However, some combination of SSH channels should produce limited moisture information, especially when used with the two window channels on the upcoming SSH-2. The most practically retrievable quantity may prove to be integrated moisture, with little or no vertical discrimination.

8.0 REFERENCES AND BIBLIOGRAPHY

Bruce, R. E., L. D. Duncan, and J. H. Pierluissi, 1977: Experimental study of the relationship between radiosonde temperatures and satellite-derived temperatures. Mon. Wea. Rev., 105, 493-496.

Burke, H. K., R. K. Crane, M. G. Fowler, and R. D. Rosen, 1978: Microwave-Infrared Retrievals. Final Report, AFGL-TR-79-0019, 70 pp, ADA065155.

Cooper, M. L., 1975: The Retrieval of Temperature Soundings from Spectral Radiance Observations Provided by the Defense Meteorological Satellite Program (DMSP), Remote Sensing of the Atmosphere, Technical Digest. Opt. Soc. Am., 19-21 March, ThB4, 1-4.

Crane, R. K., 1976: An algorithm to retrieve water vapor information from satellite measurements. NEPRF Technical Report 7-76 (ERT), 37 pp.

Dozier, J., 1980: Satellite Identificaion of Surface Radiant Temperature Fields of Subpixel Resolution. NOAA Technical Memorandum, NESS 113, 11 pp.

Duncan, L. D., 1977: Zenith angle variation of satellite thermal sounder measurements. R and D Technical Report, ECOM-5828, Atmospheric Science Laboratory, White Sands Missile Range, 7 pp. [NTIS Ref. AD-A044 660].

Gandin, L. S., 1963: Objective Analysis of Meteorological Fields. (Translated from Russian). Israel Program for Scientific Translations, Jerusalem. 242 pp. [NTIS Ref. TT 65-50007].

Hayden, C. M., W. L. Smith, and H. M. Woolf, 1981: Determination of moisture from NOAA polar orbiting satellite sounding radiances. J. Appl. Meteor., 20, 450-466.

Hillger, D. W. and T. H. Vonder Haar, 1979: An analysis of satellite infrared soundings at the mesoscale using statistical structure and correlation functions. J. Atmos. Sci., 36, 287-305.

Hillger, D. W. and T. H. Vonder Haar, 1981: Retrieval and use of high-resolution moisture and stability fields from Nimbus 6 HIRS radiances in pre-convective situations. Mon. Wea. Rev., 109, 1788-1806.

Klein, W. D., 1975: Water Vapor Data Processing Plans, DMSP Temperature Humidity Sensor, Remote Sensing of the Atmosphere, Technical Digest. Opt. Soc. Am., 19-21 March, ThB5, 1-4.

Klein, W. D., T. H. Kyle, and W. C. Smith, 1976: Special Sensor H Data Processing at AFGWC: Preliminary Results. Seventh Conference on Aerospace and Aeronautical Meteorology and Symposium on Remote Sensing from Satellites, 16-19 November, 103-108.

Matson, M. and J. Dozier, 1981: Identification of subresolution high temperature sources using a thermal IR sensor. Photogrammetric Engineering and Remote Sensing, 47, 1311-1318.

McClatchey, R. A., 1976: Satellite temperature sounding of the atmosphere: Ground truth analysis. AFGL-TR-76-0279, 39 pp, ADA038236.

McMillin, L. M. and H. E. Fleming, 1976; Atmospheric transmittance of an absorbing gas: a computationally fast and accurate transmittance model for the absorbing gases with constant mixing ratios in inhomogenous atmospheres. Appl. Opt. 15, 358-363.

McMillin, L. M., D. Q. Wark, J. M. Siomkajlo, P. G. Abel, A. Werbowetzki, L. A. Lauritson, J. A. Pritchard, D. S. Crosby, H. M. Woolf, R. C. Luebbe, M. P. Weinreb, H. E. Fleming, F. E. Bittner, and C. M. Hayden, 1973: Satellite infrared soundings from NOAA spacecraft. NOAA Technical Report, NESS 65, 112 pp. [NTIS Ref. COM-73-50936/6AS].

Minnis, P. and S. K. Cox, 1976: A polynomial representation of 6.3 μm water vapor and 4.3 μm CO_2 atmospheric transmissivities. Colorado State University, Atmospheric Science Paper No. 264, 20 pp.

Mount, W. D., B. R. Fow, D. E. Gustafson, and W. Ledsham, 1977: Error Analysis of Operational Satellite Soundings of Vertical Temperature Profiles. Final Report, AFGL-TR-77-0248, 184 pp, ADA051125.

Nagle, R. E. and J. R. Clark, 1978: Remote Sounding of the Atmosphere from Space. COSPAR, Vol. 4, 29 May - 10 June, 161-164.

Passive Microwave Sounder (SSM/T), 1977: System Summary Report. Aerojet ElectroSystems Company, Contract F-04701-75-C-0090, 133 pp.

Pryor, S. P., J. R. Gahlinger, R. C. Savage, and C. D. Hall, 1980: Derivation of High Density Temperature Fields in the Lower Stratosphere from Infrared Radiances, Preprints, International Radiation Symposium, Fort Collins, CO, 11-16 August, 65-66.

Rothman, L. S., 1978: Update of the AFGL atmospheric absorption line parameters compilation. Appl. Opt., 17, 22, 3517-3518.

Savage, R. C., 1980: SSH Moisture Sounding-Interim Report, AFGWC/TN-80/001, March, 18 pp.

Schneider, M. F. and C. J. Vesely, 1975: A Description of the DMSP Passive Microwave Temperature Sounder, Remote Sensing of the Atmosphere, Technical Digest. Opt. Soc. Am., 19-21 March, Anaheim, WA3, 1-4.

Smith, W. L., 1969: A polynomial representation of carbon dioxide and water vapor transmission. ESSA Technical Report, NESC 47, 20 pp.

Smith, W. L. and P. K. Rao, 1973: The determination of surface temperature from satellite 'window' radiation measurements. Temperature: Its Measurement and Control in Science and Industry, Volume 4, Part 3, 2251-2257.

Smith, W. L. and H. M. Woolf, 1976: The Use of Eigenvectors of Statistical Covariance Matrices for Interpreting Satellite Sounding Radiometer Observations. J. Atmos. Sci., 33, 1127-1140.

Susskind, J., 1975: Effective H_2O transmittance in the 15 μ region. Remote Sensing of the Atmosphere, Technical Digest, 19-21 March, WB6, 1-3.

Valovcin, F. R., 1980: DMSP Water Vapor Radiances - A Preliminary Evaluation. AFGL Technical Report 80-0313, 29 pp.

Valovcin, F. R., 1981: A Ground Truth Analysis of DMSP Water Vapor Radiances. AFGL-TR-81-0323, 47 pp, ADA113142.

Wachtmann, R. F., 1975: Expansion of atmospheric temperature-moisture profiles in empirical orthogonal functions for remote sensing applications. Remote Sensing of the Atmosphere, Technical Digest. Opt. Soc. Am., 19-21 March, WB5, 1-5.

Wachtmann, R. F., R. L. Weichel, W. C. Smith, 1974: Temperature Soundings from the Defense Meteorological Satellite Program. Paper Presented at Sixth Conference on Aerospace and Aeronautical Meteorology, 12-14 November, El Paso.

Weinreb, M. P. and M. L. Hill, 1980: Calculation of atmospheric radiances and brightness temperatures in infrared window channels of satellite radiometers. NOAA Technical Report, NESS 80, 43 pp. [NTIS Ref. PB80 208-119].

Weichel, R. L., 1976: Combined Microwave-Infrared Sounding Studies. AFCRL-TR-75-0572, 70 pp, ADA022681.

Yoder, J. R., 1975: Description of the Air Force infrared temperature and humidity sounder (SSH); Remote Sensing of the Atmosphere, Technical Digest. Opt. Soc. Am., 19-21 March, Anaheim, WA1, 1-4.

Zachor, A. S., 1978: Study of Temperature/Moisture Retrieval Capabilities of DMSP/SSH Sensor Channels. Final Report, AFGL-TR-78-0279, 143 pp, ADA073144.

END

FILMED

12-84

DTIC